EUROPEAN ORGANIZATION FOR NUCLEAR RESEARCH

CERN–EP/99–37

8 March 1999

Search for charginos nearly mass-degenerate with the lightest neutralino

DELPHI Collaboration

Abstract

A search for charginos with masses close to the mass of the lightest neutralino is reported, based on the data collected with the DELPHI detector at LEP from 1995 to 1997 at centre-of-mass energies between 130 and 183 GeV. The signature of a photon at high transverse momentum radiated from the initial state reduces the two-photon background to acceptable rates, thus making the mass differences between a few hundred MeV/c^2 and 3 GeV/c^2 detectable. In very nearly degenerate scenarios, the lifetime of the chargino can be large enough to produce either visible secondary vertices or decays outside the detector; therefore, quasi-stable heavy charged particles and displaced decay vertices were also searched for. No excess of events with respect to the Standard Model expectations was observed, and limits in the plane of chargino-neutralino mass difference versus chargino mass are given.

(Submitted to E. Phys. J. C)

P.Abreu[21], W.Adam[50], T.Adye[36], P.Adzic[11], Z.Albrecht[17], T.Alderweireld[2], G.D.Alekseev[16], R.Alemany[49], T.Allmendinger[17], P.P.Allport[22], S.Almehed[24], U.Amaldi[9], N.Amapane[45], S.Amato[47], E.G.Anassontzis[3], P.Andersson[44], A.Andreazza[9], S.Andringa[21], P.Antilogus[25], W-D.Apel[17], Y.Arnoud[9], B.Åsman[44], J-E.Augustin[25], A.Augustinus[9], P.Baillon[9], P.Bambade[19], F.Barao[21], G.Barbiellini[46], R.Barbier[25], D.Y.Bardin[16], G.Barker[17], A.Baroncelli[38], M.Battaglia[15], M.Baubillier[23], K-H.Becks[52], M.Begalli[6], A.Behrmann[52], P.Beilliere[8], Yu.Belokopytov[9,53], K.Belous[42], N.C.Benekos[31], A.C.Benvenuti[5], C.Berat[14], M.Berggren[25], D.Bertini[25], D.Bertrand[2], M.Besancon[39], F.Bianchi[45], M.Bigi[45], M.S.Bilenky[16], M-A.Bizouard[19], D.Bloch[10], H.M.Blom[30], M.Bonesini[27], W.Bonivento[27], M.Boonekamp[39], P.S.L.Booth[22], A.W.Borgland[4], G.Borisov[19], C.Bosio[41], O.Botner[48], E.Boudinov[30], B.Bouquet[19], C.Bourdarios[19], T.J.V.Bowcock[22], I.Boyko[16], I.Bozovic[11], M.Bozzo[13], P.Branchini[38], T.Brenke[52], R.A.Brenner[48], P.Bruckman[18], J-M.Brunet[8], L.Bugge[32], T.Buran[32], T.Burgsmueller[52], P.Buschmann[52], S.Cabrera[49], M.Caccia[27], M.Calvi[27], T.Camporesi[9], V.Canale[37], F.Carena[9], L.Carroll[22], C.Caso[13], M.V.Castillo Gimenez[49], A.Cattai[9], F.R.Cavallo[5], V.Chabaud[9], M.Chapkin[42], Ph.Charpentier[9], L.Chaussard[25], P.Checchia[35], G.A.Chelkov[16], R.Chierici[45], P.Chliapnikov[42], P.Chochula[7], V.Chorowicz[25], J.Chudoba[29], K.Cieslik[18], P.Collins[9], R.Contri[13], E.Cortina[49], G.Cosme[19], F.Cossutti[9], J-H.Cowell[22], H.B.Crawley[1], D.Crennell[36], S.Crepe[14], G.Crosetti[13], J.Cuevas Maestro[33], S.Czellar[15], M.Davenport[9], W.Da Silva[23], A.Deghorain[2], G.Della Ricca[46], P.Delpierre[26], N.Demaria[9], A.De Angelis[9], W.De Boer[17], C.De Clercq[2], B.De Lotto[46], A.De Min[35], L.De Paula[47], H.Dijkstra[9], L.Di Ciaccio[37,9], J.Dolbeau[8], K.Doroba[51], M.Dracos[10], J.Drees[52], M.Dris[31], A.Duperrin[25], J-D.Durand[9], G.Eigen[4], T.Ekelof[48], G.Ekspong[44], M.Ellert[48], M.Elsing[9], J-P.Engel[10], B.Erzen[43], M.Espirito Santo[21], E.Falk[24], G.Fanourakis[11], D.Fassouliotis[11], J.Fayot[23], M.Feindt[17], A.Fenyuk[42], P.Ferrari[27], A.Ferrer[49], E.Ferrer-Ribas[19], S.Fichet[23], A.Firestone[1], U.Flagmeyer[52], H.Foeth[9], E.Fokitis[31], F.Fontanelli[13], B.Franek[36], A.G.Frodesen[4], R.Fruhwirth[50], F.Fulda-Quenzer[19], J.Fuster[49], A.Galloni[22], D.Gamba[45], S.Gamblin[19], M.Gandelman[47], C.Garcia[49], C.Gaspar[9], M.Gaspar[47], U.Gasparini[35], Ph.Gavillet[9], E.N.Gazis[31], D.Gele[10], N.Ghodbane[25], I.Gil[49], F.Glege[52], R.Gokieli[9,51], B.Golob[43], G.Gomez-Ceballos[40], P.Goncalves[21], I.Gonzalez Caballero[40], G.Gopal[36], L.Gorn[1,54], M.Gorski[51], Yu.Gouz[42], V.Gracco[13], J.Grahl[1], E.Graziani[38], C.Green[22], H-J.Grimm[17], P.Gris[39], G.Grosdidier[19], K.Grzelak[51], M.Gunther[48], J.Guy[36], F.Hahn[9], S.Hahn[52], S.Haider[9], A.Hallgren[48], K.Hamacher[52], J.Hansen[32], F.J.Harris[34], V.Hedberg[24], S.Heising[17], J.J.Hernandez[49], P.Herquet[2], H.Herr[9], T.L.Hessing[34], J.-M.Heuser[52], E.Higon[49], S-O.Holmgren[44], P.J.Holt[34], S.Hoorelbeke[2], M.Houlden[22], K.Huet[2], G.J.Hughes[22], K.Hultqvist[44], J.N.Jackson[22], R.Jacobsson[9], P.Jalocha[9], R.Janik[7], Ch.Jarlskog[24], G.Jarlskog[24], P.Jarry[39], B.Jean-Marie[19], E.K.Johansson[44], P.Jonsson[25], C.Joram[9], P.Juillot[10], F.Kapusta[23], K.Karafasoulis[11], S.Katsanevas[25], E.C.Katsoufis[31], R.Keranen[17], B.P.Kersevan[43], B.A.Khomenko[16], N.N.Khovanski[16], A.Kiiskinen[15], B.King[22], A.Kinvig[22], N.J.Kjaer[30], O.Klapp[52], H.Klein[9], P.Kluit[30], P.Kokkinias[11], M.Koratzinos[9], V.Kostioukhine[42], C.Kourkoumelis[3], O.Kouznetsov[39], M.Krammer[50], E.Kriznic[43], P.Krstic[11], Z.Krumstein[16], P.Kubinec[7], J.Kurowska[51], K.Kurvinen[15], C.Lacasta[49], J.W.Lamsa[1], D.W.Lane[1], P.Langefeld[52], V.Lapin[42], J-P.Laugier[39], R.Lauhakangas[15], G.Leder[50], F.Ledroit[14], V.Lefebure[2], L.Leinonen[44], A.Leisos[11], R.Leitner[29], G.Lenzen[52], V.Lepeltier[19], T.Lesiak[18], M.Lethuillier[39], J.Libby[34], D.Liko[9], A.Lipniacka[44], I.Lippi[35], B.Loerstad[24], J.G.Loken[34], J.H.Lopes[47], J.M.Lopez[40], R.Lopez-Fernandez[14], D.Loukas[11], P.Lutz[39], L.Lyons[34], J.MacNaughton[50], J.R.Mahon[6], A.Maio[21], A.Malek[52], T.G.M.Malmgren[44], S.Maltezos[31], V.Malychev[16], F.Mandl[50], J.Marco[40], R.Marco[40], B.Marechal[47], M.Margoni[35], J-C.Marin[9], C.Mariotti[9], A.Markou[11], C.Martinez-Rivero[19], F.Martinez-Vidal[49], S.Marti i Garcia[9], J.Masik[12], N.Mastroyiannopoulos[11], F.Matorras[40], C.Matteuzzi[27], G.Matthiae[37], F.Mazzucato[35], M.Mazzucato[35], M.Mc Cubbin[22], R.Mc Kay[1], R.Mc Nulty[22], G.Mc Pherson[22], C.Meroni[27], W.T.Meyer[1], E.Migliore[45], L.Mirabito[25], W.A.Mitaroff[50], U.Mjoernmark[24], T.Moa[44], M.Moch[17], R.Moeller[28], K.Moenig[9], M.R.Monge[13], X.Moreau[23], P.Morettini[13], G.Morton[34], U.Mueller[52], K.Muenich[52], M.Mulders[30], C.Mulet-Marquis[14], R.Muresan[24], W.J.Murray[36], B.Muryn[14,18], G.Myatt[34], T.Myklebust[32], F.Naraghi[14], F.L.Navarria[5], S.Navas[49], K.Nawrocki[51], P.Negri[27], S.Nemecek[12], N.Neufeld[9], N.Neumeister[50], R.Nicolaidou[39], B.S.Nielsen[28], M.Nikolenko[10,16], V.Nomokonov[15], A.Normand[22], A.Nygren[24], V.Obraztsov[42], A.G.Olshevski[16], A.Onofre[21], R.Orava[15], G.Orazi[10], K.Osterberg[15], A.Ouraou[39], M.Paganoni[27], S.Paiano[5], R.Pain[23], R.Paiva[21], J.Palacios[34], H.Palka[18], Th.D.Papadopoulou[31], K.Papageorgiou[11], L.Pape[9], C.Parkes[9], F.Parodi[13], U.Parzefall[22], A.Passeri[38], O.Passon[52], M.Pegoraro[35], L.Peralta[21], M.Pernicka[50], A.Perrotta[5], C.Petridou[46], A.Petrolini[13], H.T.Phillips[36], F.Pierre[39], M.Pimenta[21], E.Piotto[27], T.Podobnik[43], M.E.Pol[6], G.Polok[18], P.Poropat[46], V.Pozdniakov[16], P.Privitera[37], N.Pukhaeva[16], A.Pullia[27], D.Radojicic[34], S.Ragazzi[27], H.Rahmani[31], D.Rakoczy[50], P.N.Ratoff[20], A.L.Read[32], P.Rebecchi[9], N.G.Redaelli[27], M.Regler[50], D.Reid[30], R.Reinhardt[52], P.B.Renton[34], L.K.Resvanis[3], F.Richard[19], J.Ridky[12], G.Rinaudo[45], O.Rohne[32], A.Romero[45], P.Ronchese[35], E.I.Rosenberg[1], P.Rosinsky[7], P.Roudeau[19], T.Rovelli[5], Ch.Royon[39], V.Ruhlmann-Kleider[39], A.Ruiz[40], H.Saarikko[15], Y.Sacquin[39], A.Sadovsky[16], G.Sajot[14], J.Salt[49], D.Sampsonidis[11], M.Sannino[13], H.Schneider[17], Ph.Schwemling[23], B.Schwering[52], U.Schwickerath[17], M.A.E.Schyns[52], F.Scuri[46], P.Seager[20], Y.Sedykh[16], A.M.Segar[34], R.Sekulin[36], R.C.Shellard[6], A.Sheridan[22], M.Siebel[52], L.Simard[39], F.Simonetto[35], A.N.Sisakian[16], G.Smadja[25], N.Smirnov[42], O.Smirnova[24], G.R.Smith[36],

A.Sopczak[17], R.Sosnowski[51], T.Spassov[21], E.Spiriti[38], P.Sponholz[52], S.Squarcia[13], D.Stampfer[50], C.Stanescu[38], S.Stanic[43], K.Stevenson[34], A.Stocchi[19], J.Strauss[50], R.Strub[10], B.Stugu[4], M.Szczekowski[51], M.Szeptycka[51], T.Tabarelli[27], F.Tegenfeldt[48], F.Terranova[27], J.Thomas[34], J.Timmermans[30], N.Tinti[5], L.G.Tkatchev[16], S.Todorova[10], A.Tomaradze[2], B.Tome[21], A.Tonazzo[9], L.Tortora[38], G.Transtromer[24], D.Treille[9], G.Tristram[8], M.Trochimczuk[51], C.Troncon[27], A.Tsirou[9], M-L.Turluer[39], I.A.Tyapkin[16], S.Tzamarias[11], O.Ullaland[9], V.Uvarov[42], G.Valenti[5], E.Vallazza[46], C.Vander Velde[2], G.W.Van Apeldoorn[30], P.Van Dam[30], J.Van Eldik[30], A.Van Lysebetten[2], I.Van Vulpen[30], N.Vassilopoulos[34], G.Vegni[27], L.Ventura[35], W.Venus[36,9], F.Verbeure[2], M.Verlato[35], L.S.Vertogradov[16], V.Verzi[37], D.Vilanova[39], L.Vitale[46], E.Vlasov[42], A.S.Vodopyanov[16], C.Vollmer[17], G.Voulgaris[3], V.Vrba[12], H.Wahlen[52], C.Walck[44], C.Weiser[17], D.Wicke[52], J.H.Wickens[2], G.R.Wilkinson[9], M.Winter[10], M.Witek[18], G.Wolf[9], J.Yi[1], O.Yushchenko[42], A.Zaitsev[42], A.Zalewska[18], P.Zalewski[51], D.Zavrtanik[43], E.Zevgolatakos[11], N.I.Zimin[16,24], G.C.Zucchelli[44], G.Zumerle[35]

[1] Department of Physics and Astronomy, Iowa State University, Ames IA 50011-3160, USA
[2] Physics Department, Univ. Instelling Antwerpen, Universiteitsplein 1, BE-2610 Wilrijk, Belgium
and IIHE, ULB-VUB, Pleinlaan 2, BE-1050 Brussels, Belgium
and Faculté des Sciences, Univ. de l'Etat Mons, Av. Maistriau 19, BE-7000 Mons, Belgium
[3] Physics Laboratory, University of Athens, Solonos Str. 104, GR-10680 Athens, Greece
[4] Department of Physics, University of Bergen, Allégaten 55, NO-5007 Bergen, Norway
[5] Dipartimento di Fisica, Università di Bologna and INFN, Via Irnerio 46, IT-40126 Bologna, Italy
[6] Centro Brasileiro de Pesquisas Físicas, rua Xavier Sigaud 150, BR-22290 Rio de Janeiro, Brazil
and Depto. de Física, Pont. Univ. Católica, C.P. 38071 BR-22453 Rio de Janeiro, Brazil
and Inst. de Física, Univ. Estadual do Rio de Janeiro, rua São Francisco Xavier 524, Rio de Janeiro, Brazil
[7] Comenius University, Faculty of Mathematics and Physics, Mlynska Dolina, SK-84215 Bratislava, Slovakia
[8] Collège de France, Lab. de Physique Corpusculaire, IN2P3-CNRS, FR-75231 Paris Cedex 05, France
[9] CERN, CH-1211 Geneva 23, Switzerland
[10] Institut de Recherches Subatomiques, IN2P3 - CNRS/ULP - BP20, FR-67037 Strasbourg Cedex, France
[11] Institute of Nuclear Physics, N.C.S.R. Demokritos, P.O. Box 60228, GR-15310 Athens, Greece
[12] FZU, Inst. of Phys. of the C.A.S. High Energy Physics Division, Na Slovance 2, CZ-180 40, Praha 8, Czech Republic
[13] Dipartimento di Fisica, Università di Genova and INFN, Via Dodecaneso 33, IT-16146 Genova, Italy
[14] Institut des Sciences Nucléaires, IN2P3-CNRS, Université de Grenoble 1, FR-38026 Grenoble Cedex, France
[15] Helsinki Institute of Physics, HIP, P.O. Box 9, FI-00014 Helsinki, Finland
[16] Joint Institute for Nuclear Research, Dubna, Head Post Office, P.O. Box 79, RU-101 000 Moscow, Russian Federation
[17] Institut für Experimentelle Kernphysik, Universität Karlsruhe, Postfach 6980, DE-76128 Karlsruhe, Germany
[18] Institute of Nuclear Physics and University of Mining and Metalurgy, Ul. Kawiory 26a, PL-30055 Krakow, Poland
[19] Université de Paris-Sud, Lab. de l'Accélérateur Linéaire, IN2P3-CNRS, Bât. 200, FR-91405 Orsay Cedex, France
[20] School of Physics and Chemistry, University of Lancaster, Lancaster LA1 4YB, UK
[21] LIP, IST, FCUL - Av. Elias Garcia, 14-1^{o}, PT-1000 Lisboa Codex, Portugal
[22] Department of Physics, University of Liverpool, P.O. Box 147, Liverpool L69 3BX, UK
[23] LPNHE, IN2P3-CNRS, Univ. Paris VI et VII, Tour 33 (RdC), 4 place Jussieu, FR-75252 Paris Cedex 05, France
[24] Department of Physics, University of Lund, Sölvegatan 14, SE-223 63 Lund, Sweden
[25] Université Claude Bernard de Lyon, IPNL, IN2P3-CNRS, FR-69622 Villeurbanne Cedex, France
[26] Univ. d'Aix - Marseille II - CPP, IN2P3-CNRS, FR-13288 Marseille Cedex 09, France
[27] Dipartimento di Fisica, Università di Milano and INFN, Via Celoria 16, IT-20133 Milan, Italy
[28] Niels Bohr Institute, Blegdamsvej 17, DK-2100 Copenhagen Ø, Denmark
[29] NC, Nuclear Centre of MFF, Charles University, Areal MFF, V Holesovickach 2, CZ-180 00, Praha 8, Czech Republic
[30] NIKHEF, Postbus 41882, NL-1009 DB Amsterdam, The Netherlands
[31] National Technical University, Physics Department, Zografou Campus, GR-15773 Athens, Greece
[32] Physics Department, University of Oslo, Blindern, NO-1000 Oslo 3, Norway
[33] Dpto. Fisica, Univ. Oviedo, Avda. Calvo Sotelo s/n, ES-33007 Oviedo, Spain
[34] Department of Physics, University of Oxford, Keble Road, Oxford OX1 3RH, UK
[35] Dipartimento di Fisica, Università di Padova and INFN, Via Marzolo 8, IT-35131 Padua, Italy
[36] Rutherford Appleton Laboratory, Chilton, Didcot OX11 OQX, UK
[37] Dipartimento di Fisica, Università di Roma II and INFN, Tor Vergata, IT-00173 Rome, Italy
[38] Dipartimento di Fisica, Università di Roma III and INFN, Via della Vasca Navale 84, IT-00146 Rome, Italy
[39] DAPNIA/Service de Physique des Particules, CEA-Saclay, FR-91191 Gif-sur-Yvette Cedex, France
[40] Instituto de Fisica de Cantabria (CSIC-UC), Avda. los Castros s/n, ES-39006 Santander, Spain
[41] Dipartimento di Fisica, Università degli Studi di Roma La Sapienza, Piazzale Aldo Moro 2, IT-00185 Rome, Italy
[42] Inst. for High Energy Physics, Serpukov P.O. Box 35, Protvino, (Moscow Region), Russian Federation
[43] J. Stefan Institute, Jamova 39, SI-1000 Ljubljana, Slovenia and Laboratory for Astroparticle Physics,
Nova Gorica Polytechnic, Kostanjeviska 16a, SI-5000 Nova Gorica, Slovenia,
and Department of Physics, University of Ljubljana, SI-1000 Ljubljana, Slovenia
[44] Fysikum, Stockholm University, Box 6730, SE-113 85 Stockholm, Sweden
[45] Dipartimento di Fisica Sperimentale, Università di Torino and INFN, Via P. Giuria 1, IT-10125 Turin, Italy
[46] Dipartimento di Fisica, Università di Trieste and INFN, Via A. Valerio 2, IT-34127 Trieste, Italy
and Istituto di Fisica, Università di Udine, IT-33100 Udine, Italy
[47] Univ. Federal do Rio de Janeiro, C.P. 68528 Cidade Univ., Ilha do Fundão BR-21945-970 Rio de Janeiro, Brazil
[48] Department of Radiation Sciences, University of Uppsala, P.O. Box 535, SE-751 21 Uppsala, Sweden
[49] IFIC, Valencia-CSIC, and D.F.A.M.N., U. de Valencia, Avda. Dr. Moliner 50, ES-46100 Burjassot (Valencia), Spain
[50] Institut für Hochenergiephysik, Österr. Akad. d. Wissensch., Nikolsdorfergasse 18, AT-1050 Vienna, Austria
[51] Inst. Nuclear Studies and University of Warsaw, Ul. Hoza 69, PL-00681 Warsaw, Poland
[52] Fachbereich Physik, University of Wuppertal, Postfach 100 127, DE-42097 Wuppertal, Germany
[53] On leave of absence from IHEP Serpukhov
[54] Now at University of Florida

1 Introduction

Supersymmetry (SUSY) [1] is an appealing theory which answers some well-known outstanding questions of the Standard Model (SM), at the expense of introducing supersymmetric partners of the known particles (sparticles). The most well-studied example of supersymmetry is the minimal supersymmetric extension of the SM (the MSSM). If the R-parity quantum number is conserved, as often assumed, there must exist a lightest supersymmetric particle (LSP) which is stable and remains after any SUSY decay chain. Such an LSP is expected to be neutral and weakly interacting [2]. The usual way of searching for SUSY particles heavier than the LSP in e^+e^- interactions is therefore to look for visible particles accompanied by the missing energy carried away by two or more LSP's. This works whenever the mass difference between the produced sparticle and the LSP is large enough to leave some sizeable amount of energy for the visible final state particles. Typically, the searches carried out so far at LEP in the different SUSY channels go down to mass differences of a few GeV/c^2. Previous DELPHI searches at LEP2 have resulted in limits on the production of charginos, neutralinos, sleptons and $\tilde{\mathrm{b}}$ and $\tilde{\mathrm{t}}$ squarks in the MSSM, valid when the mass difference between the sparticles searched for and the LSP (usually the lightest neutralino) is above 3 to 5 GeV/c^2 [3,4]. For smaller mass differences, the only limits available so far are those derived from the precise measurement of the Z width at LEP1; in particular charginos lighter than about $M_{\mathrm{Z}}/2$ are excluded, irrespective of their field content [5,6].

The search for charginos and neutralinos is essential to constrain SUSY. It is therefore of paramount importance to make sure that they have not been missed because of possible small mass differences amongst them. Such small mass differences are rather unlikely in the MSSM if the masses of the gauginos are assumed to be all the same at some grand unified scale, as expected in supergravity (SUGRA) models. In such models the lightest chargino and the two lightest neutralinos can have nearly the same mass only if those gaugino masses are unnaturally large (above 1 TeV/c^2). However, since no direct experimental support for those models has been found so far, it is reasonable to also consider models without the SUGRA assumptions. In particular, there are interesting theoretical string-motivated scenarios which explicitly prefer the non-unification of the gaugino masses at the GUT scale [7] and in which is quite likely that the lightest chargino and the lightest neutralino have nearly equal masses [8]. Recently, another model appeared in which the usual GUT relations are modified [**?**], again leading to scenarios in which small mass differences between the lightest gauginos are likely.

The region of low mass difference is experimentally challenging. If the chargino-neutralino mass difference $\Delta M^{\pm} = M_{\tilde{\chi}_1^{\pm}} - M_{\tilde{\chi}_1^0}$ is below the mass of the pion, the lifetime of the chargino can be so long that it passes through the entire detector before decaying. In DELPHI this can be covered by a search for heavy charged particles identified with the Cherenkov detectors and/or because of their anomalously high ionization in the gas chambers. Mass differences of a few hundred MeV/c^2 may be observed by looking for reconstructed secondary vertices from a chargino decay inside the detector but significantly displaced from the main interaction point.

When $\Delta M^{\pm}$ increases, the chargino decay length becomes so short that the decay vertex can hardly be distinguished from the production one. However, as long as $\Delta M^{\pm}$ remains below a few GeV/c^2, the visible particles carry only a small fraction of the parent energy. A minimum visible transverse momentum is usually required to reject two-photon interactions. This may result in an almost complete loss of efficiency for chargino decays. On the other hand, some transverse momentum requirement is necessary because the

two-photon cross-section is orders of magnitude higher than any signal searched for at LEP2. Here a suggestion by Chen, Drees and Gunion [9] is applied to search for these charginos at low $\Delta M^{\pm}$ (a similar technique was already applied in the search for nearly degenerate lepton doublets at PEP [10]). If one considers the events accompanied by a hard photon from Initial State Radiation (ISR), then the two-photon background can be kept small by choosing the photon transverse energy to be greater than

$$(E_\gamma^T)^{\min} = \sqrt{s} \cdot \frac{\sin\theta_{\min}}{1+\sin\theta_{\min}} \quad , \tag{1}$$

where $\theta_{\min}$ is the lowest polar angle accessible in the detector. If an ISR photon with a transverse energy above $(E_\gamma^T)^{\min}$ is radiated from a two-photon event then, typically, one of the final state electrons, which usually escape undetected in the beam pipe, should be deflected at an angle larger than $\theta_{\min}$, thus allowing the identification of the event as background. Such a selection gives a low efficiency since only a small fraction of the SUSY events have an ISR photon with $E_\gamma^T > (E_\gamma^T)^{\min}$. On the other hand, the presence of the high energy photon in the detector substantially increases the otherwise low trigger efficiency for these decays with only a few soft visible particles.

This paper first explores the feasibility of a search at LEP2 for charginos or second lightest neutralinos nearly mass-degenerate with the lightest neutralino. In the case of the second lightest neutralino (for which the relevant mass difference is $\Delta M^0 = M_{\tilde{\chi}_2^0} - M_{\tilde{\chi}_1^0}$) it will be shown that a search at LEP2 is either impossible or quite difficult, at least for most of the values of ΔM^0 of interest here. Instead, a search for mass-degenerate charginos was found to be feasible, and was realized using the data collected by the DELPHI experiment. For sensitivity in the case of long chargino lifetimes two alternative searches were used, as described in section 4: one is the search for heavy stable charged particles described in [11], and the other is a modified version of a search for secondary vertices [12] with reconstructed incoming and outgoing tracks (kinks). The search which exploits the ISR signature to cover the mass differences between 0.3 and 3 GeV/c^2 was specifically designed for this work and is discussed in section 5.

2 Data samples and event generators

A detailed description of the working DELPHI detector can be found in [13]. The trajectories of the charged particles are reconstructed in the 1.2 T magnetic field by a system of cylindrical tracking chambers. The most relevant for the analyses reported here are the Silicon Tracker, the Inner Detector (ID), and the Time Projection Chamber (TPC). The Silicon Tracker is composed of the Vertex Detector (VD) in the barrel and the ministrips and pixels of the Very Forward Tracker (VFT) at low polar angles (θ); it covers the range between 10° and 170° in θ and radii down to 6.3 cm from the beam. The ID covers polar angles down to 15° (165°). The TPC tracks particles between the radii of 29 and 122 cm, with at least three pad rows crossed if θ is between 20° and 160°. The electromagnetic calorimeters are the High density Projection Chamber (HPC) in the barrel ($40° < \theta < 140°$), the Forward ElectroMagnetic Calorimeter (FEMC) in the forward regions ($11° < \theta < 36°$ and $144° < \theta < 169°$) and the Small angle TIle Calorimeter (STIC) in the very forward part (down to 1.66° from the beam axis). In front of the STIC, which is also the luminometer of DELPHI, have been placed two planes of scintillators (Veto Counters [14]) used to detect charged particles which enter the calorimeter. Excellent particle identification is provided by the Ring Imaging CHerenkov (RICH) detectors,

equipped with two different radiators (liquid and gas) with different refractive index, and thus different momentum thresholds.

During the high energy runs of LEP in 1995-97, DELPHI collected data at centre-of-mass energies of approximately 130, 136, 161, 172 and 183 GeV. Only the runs in which the relevant subdetectors worked correctly were taken into account for each analysis. The luminosities used at the different energies in the analyses considered here are approximately 6, 6, 10, 10 and 54 pb^{-1} respectively. The data at 130 and 136 GeV where not searched for kinks; in the search for soft particles accompanied by ISR only 50 pb^{-1} of the run at 183 GeV could be used, mainly because of some temporary degradation of the quality of the data collected by the HPC and FEMC calorimeters, which are fundamental for that analysis.

To evaluate the signal efficiency and the background contamination, events were generated using several different programs, all relying on JETSET 7.4 [15] for quark fragmentation. All the events generated were passed through a complete simulation of the DELPHI detector [16], and then processed in exactly the same way as the real data.

The program SUSYGEN [17], which includes initial and final state photon radiation, was used to simulate all signal events. The implementation of the decay widths (i.e. branching ratios and lifetimes) in SUSYGEN at low $\Delta M^{\pm}$ has been modified in order to reproduce the results of the analytical calculations reported in [8] and [18].

For the Standard Model background, several samples of the different final states were generated with statistics which were typically well above those expected (although some of the two-photon samples, especially at the lowest centre-of-mass energies studied here, were originally simulated with statistics only slightly higher than the one expected). Annihiliation of $\mathrm{e^+e^-}$ into a virtual Z/γ, including ISR, were generated with PYTHIA [15]. This generator was also used for four-fermion processes. For the two-photon collisions, the generator of Berends, Daverveldt and Kleiss (BDK) [19] was used for the leptonic final states. In this generator the $(\mathrm{e^+e^-})\mu^+\mu^-$ and $(\mathrm{e^+e^-})\tau^+\tau^-$ final states include also the simulation of the ISR photon, while in $(\mathrm{e^+e^-})\mathrm{e^+e^-}$ ISR is not implemented. In the two-photon interactions leading to hadronic final states, the QCD and VDM parts were simulated with the TWOGAM [20] generator, which had no ISR. BDK, with ISR, was used for the QPM part. Although not used for the computation of the background, QPM events were also generated using the TWOGAM generator, to study the differences between the two programs, in particular biases due to the absence of ISR; after the comparison, there was evidence that having no ISR in some of the two-photon samples can lead to an underestimation of the background in the search which uses the ISR tag.

3 Chargino and neutralino production and decay at low ΔM

The higgsino and gaugino sector of the MSSM can be described in terms of four parameters: the ratio $\tan\beta$ of the two Higgs vacuum expectation values, the Higgs mixing parameter μ, the $SU(2)$ gaugino mass M_2 and the $U(1)$ gaugino mass M_1. In the models with gaugino mass unification at the GUT scale, there is a relation between M_1 and M_2

$$M_1 = \frac{5}{3}\tan^2\theta_W \cdot M_2 \simeq 0.5 \cdot M_2 \quad . \tag{2}$$

However, it has been already anticipated that this unification is not strictly necessary in the theory and there are several models without it, in particular the SUSY-string scenario

proposed in [8]. The definition

$$M_1 = R_f \cdot \frac{5}{3} \tan^2 \theta_W \cdot M_2 \quad , \tag{3}$$

will be used, so that any value of R_f different from 1 indicates how much the model deviates from the gaugino mass unification hypothesis.

In the MSSM there are two charginos ($\tilde{\chi}_1^{\pm}$ and $\tilde{\chi}_2^{\pm}$). These mass eigenstates are linear combinations of the two interaction eigenstates, the wino and the charged higgsino. There are also four neutralinos, linear combinations of the neutral eigenstates. In the following it will be assumed that the lightest neutralino is the LSP.

The lightest chargino gets almost the same mass as such an LSP in two cases [8]:

1. Low $|\mu|$, large $M_{1,2}$ scenario: $\tilde{\chi}_1^0$ and $\tilde{\chi}_1^+$ are both higgsino-like and nearly degenerate, with masses $\sim |\mu|$;
2. High $|\mu|$, low M_2 scenario: the $\tilde{\chi}_1^0$ and the $\tilde{\chi}_1^+$ are both gaugino-like and nearly degenerate with masses $\sim M_2$. In this scenario, in order to have $\Delta M^{\pm}$ around 1 GeV/c^2 or smaller, R_f in eq. (3) must be larger than or equal to 2.

In the first scenario, the second lightest neutralino is also almost mass-degenerate with the lightest neutralino, with a mass splitting which is sligtly larger than that of the lightest chargino. The same is true also for the second scenario, but only for $R_f \simeq 2$.

3.1 Cross-sections

The predicted $e^+e^- \to \tilde{\chi}_1^+ \tilde{\chi}_1^-$ and $e^+e^- \to \tilde{\chi}_1^0 \tilde{\chi}_2^0$ cross-sections [17] at the centre-of-mass energy of 183 GeV are shown in figures 1 and 2, respectively, as functions of the $\tilde{\chi}_1^{\pm}$ and $\tilde{\chi}_2^0$ masses. That value of the centre-of-mass energy is taken as example, since the behaviour is similar for all energies studied. In both figures, the upper plot refers to the higgsino cross-section and the lower plot to the gaugino one.

For the neutralinos, the $e^+e^- \to \tilde{\chi}_1^0 \tilde{\chi}_1^0$ and $e^+e^- \to \tilde{\chi}_2^0 \tilde{\chi}_2^0$ cross-sections are much smaller than the $e^+e^- \to \tilde{\chi}_1^0 \tilde{\chi}_2^0$ one, shown in figure 2. This last process is the only one considered in the following for the production of neutralinos at LEP2.

The widths of the bands arise from a variation of $\tan\beta$ from 1 to 50, M_2 and $|\mu|$ below 100 TeV/c^2, R_f between 1 and 10. The higgsino cross-sections are quite stable when varying R_f, and also the values assumed by the charged gaugino cross-sections do not deviate by more than 5% if R_f moves in that range. In the chargino production, the exchange of sfermions in the t-channel interferes destructively with the s-channel production, lowering the gaugino cross-section at small values of $M_{\tilde{\nu}}$. On the contrary, in the neutralino production the interference is constructive and the gaugino cross-sections are enhanced at low $M_{\tilde{e}}$. In all the figures the mass of the relevant scalar lepton has been varied from $M_{\tilde{\chi}}$ to 1 TeV/c^2.

The chargino cross-section, in the approximation of large scalar masses, is roughly three times larger in the gaugino-like scenario than in the higgsino-like one. On the contrary, the $e^+e^- \to \tilde{\chi}_1^0 \tilde{\chi}_2^0$ cross-section in the gaugino-like scenario is typically several orders of magnitude smaller than in the higgsino one, certainly out of reach of the luminosity planned at LEP2.

3.2 Branching ratios and lifetimes

The partial decay widths of the chargino in SUSYGEN have been modified in order to account for the decays into a neutralino and one, two or three pions, according to analytical

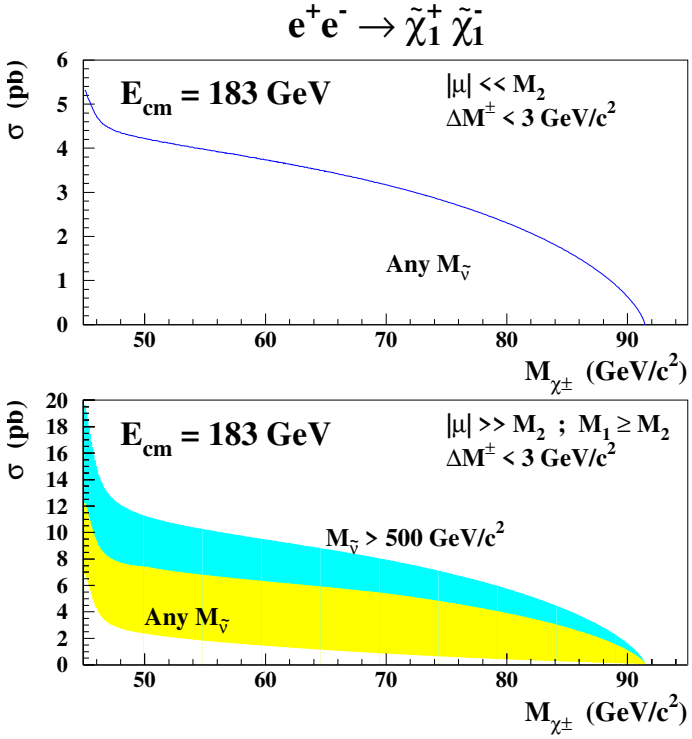

Figure 1: Predicted $e^+e^- \to \tilde{\chi}_1^+\tilde{\chi}_1^-$ cross-sections at the centre-of-mass energy of 183 GeV as a function of the mass of the chargino. The upper plot refers to the $|\mu| \ll M_2$ higgsino-like scenario; the lower plot to the $M_2 \ll |\mu|$ gaugino-like scenario. The widths of the bands allow for a variation of M_1, M_2 and μ so that $0 < \Delta M^{\pm} < 3$ GeV/c^2; $1 < \tan\beta < 50$; $M_2 \leq 2M_1 \leq 10M_2$; $M_{\tilde{\nu}} > M_{\tilde{\chi}_1^{\pm}}$ (the upper part of the gaugino band displays separately the points corresponding to $M_{\tilde{\nu}} > 500$ GeV/c^2).

calculations [8,18]. These calculations use the form factors of the low mass hadronic resonances to determine the hadronic width for $0 < \Delta M^{\pm} < 2$ GeV/c^2. This treatment has been verified [8] to describe correctly the τ decays, i.e. decays with $\Delta M = m_\tau$.

Figure 3a and b show the leptonic and hadronic branching ratios computed for a 50 GeV/c^2 charged higgsino with a mass between 100 MeV/c^2 and 5 GeV/c^2 above that of the lightest neutralino. In the plot of the hadronic modes, the decays into a $\tilde{\chi}_1^0$ and one, two or three π, which contribute to the total $\tilde{\chi}_1^+ \to \tilde{\chi}_1^0 q\bar{q}$ width, are shown separately. For a gaugino, the leptonic width is enhanced for low $M_{\tilde{\nu}}$ because of the sneutrino mediated decays, and this was taken into account in the analysis.

Figure 3c shows the lifetime of the same chargino as a function of $\Delta M^{\pm}$. The figure clearly shows the step caused by the onset of the dominating $\tilde{\chi}_1^+ \to \tilde{\chi}_1^0\pi^+$ two body decay. The chargino lifetime and branching ratios depend strongly on $\Delta M^{\pm}$ and relatively little on the SUSY scenario, as long as scalar exchange can be neglected. For low $M_{\tilde{\nu}}$, charged gauginos get a shorter lifetime, and this was also taken into account in the analysis.

Figure 4 shows the exclusive branching ratios of the second lightest neutralino as a function of ΔM^0, in the two scenarios which allow almost degenerate states. Unlike the chargino case, there is now a strong model dependence of the decay widths. As already mentioned, the only neutralino scenario with a sufficient cross-section to be searched for is the higgsino one. In this scenario the rate of the radiative decay $\tilde{\chi}_2^0 \to \tilde{\chi}_1^0\gamma$ increases in the low ΔM^0 region of interest here. Thus a large fraction of the $\tilde{\chi}_2^0$ decays yield either a low

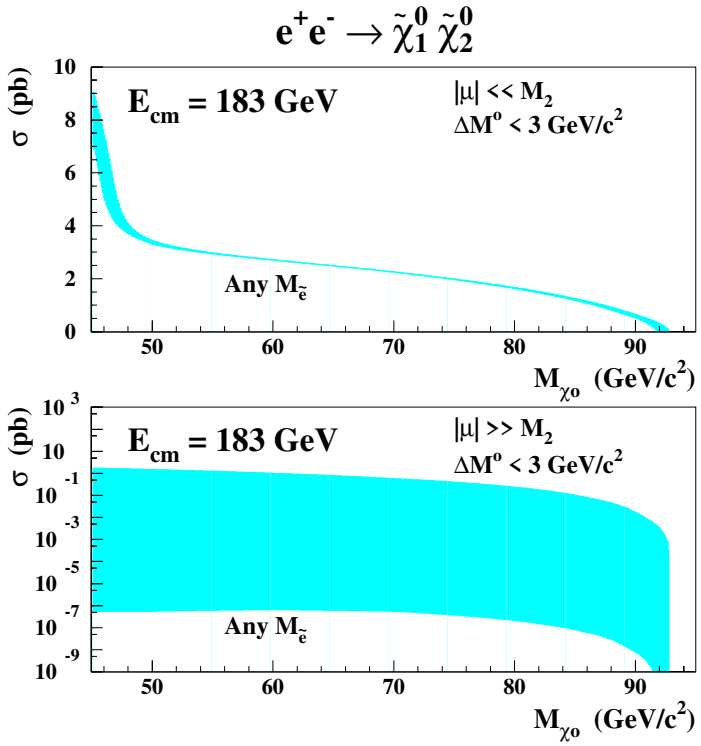

Figure 2: Predicted $e^+e^- \to \tilde{\chi}_1^0\tilde{\chi}_2^0$ cross-sections at the centre-of-mass energy of 183 GeV and as a function of the $\tilde{\chi}_2^0$ mass. The upper plot refers to $|\mu| \ll M_2$ higgsino-like scenario; the lower plot refers to the $M_2 \ll |\mu|$ gaugino like scenario. The width of the bands allows for a variation of M_2, M_1 and μ so that for any given mass of the second neutralino $0 < \Delta M^0 < 3$ GeV/c^2; $1 < \tan\beta < 50$; $1 < R_f < 10$ ($R_f \simeq 2$ for the gaugino); $M_{\tilde{e}} > M_{\tilde{\chi}_2^0}$.

energy photon or a pair of neutrinos, in addition to the LSP. Since it is difficult to identify photons below about 1 GeV in the detector and distinguish them from background, both decay modes can be considered invisible for practical purposes. For these reasons the present work has been limited to charginos, leaving neutralinos aside.

4 Search for long-lived charginos

Two methods were used to look for charginos with a visible decay length: the search for heavy stable charged particles and the search for decay vertices inside the detector. Both searches are described in this section.

4.1 Heavy stable charged particles

Heavy stable or almost stable charged particles are identified through their anomalously high specific ionization in the TPC or by the absence of Cherenkov light produced in the two radiators of the barrel RICH. The leptonic selection described in [11] is the one used for the present analysis. The efficiency of this selection for pair-produced heavy charged particles, traversing the full depth of the detector, is given in [11]. Figure 5 shows the efficiency for selecting a single heavy charged particle as a function of its mass and of the

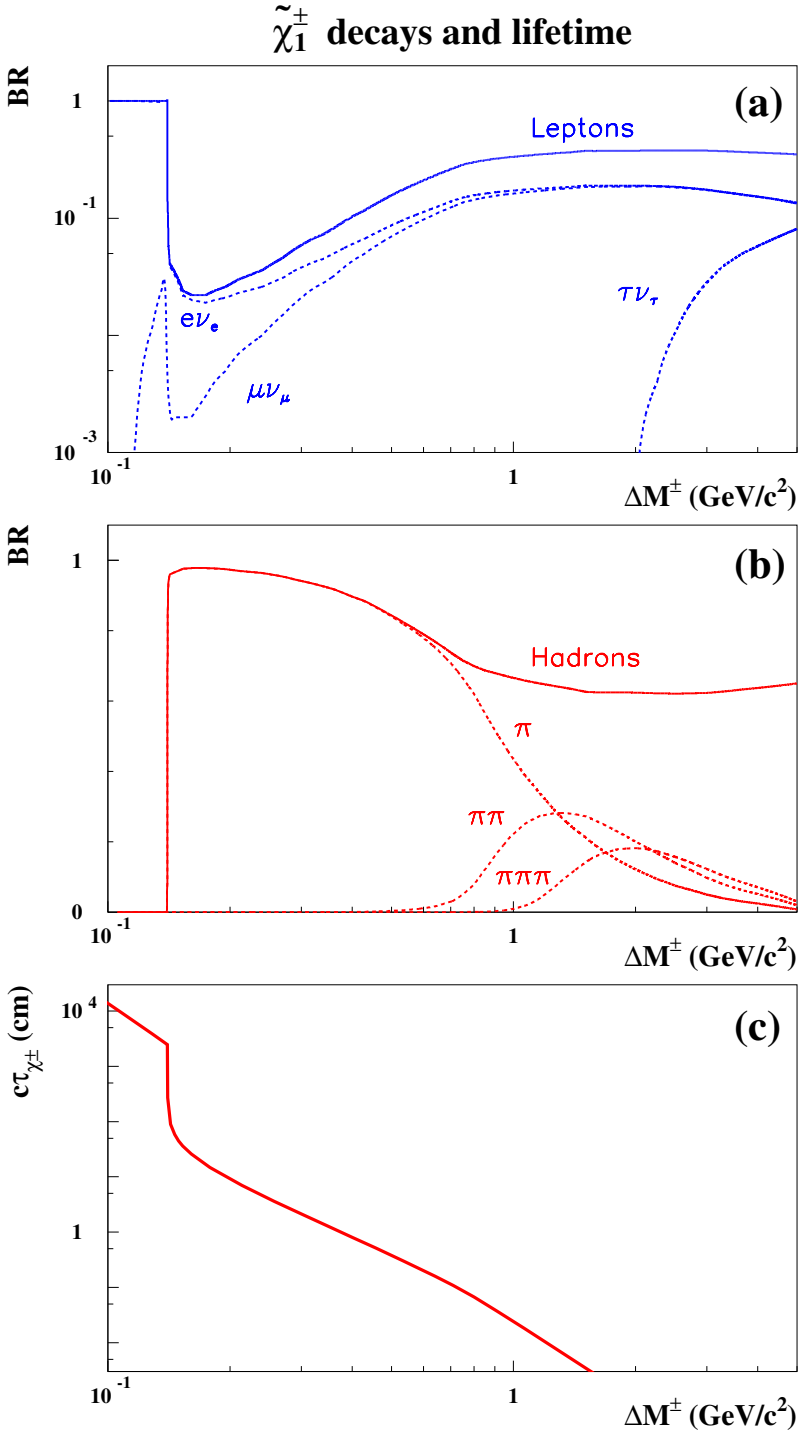

Figure 3: Predicted (a) leptonic and (b) hadronic branching ratios and (c) lifetime of a 50 GeV/c^2 chargino (higgsino) decaying into a $\tilde{\chi}_1^0$ plus standard particles, as a function of the mass difference between the $\tilde{\chi}_1^+$ and the $\tilde{\chi}_1^0$. Similar decay modes are predicted for the gaugino scenario in the approximation of large $M_{\tilde{\nu}}$, which makes the contribution of the $\tilde{\nu}$ mediated decays negligible. For smaller $M_{\tilde{\nu}}$, the leptonic decays of the charged gaugino are enhanced and the lifetime gets shorter.

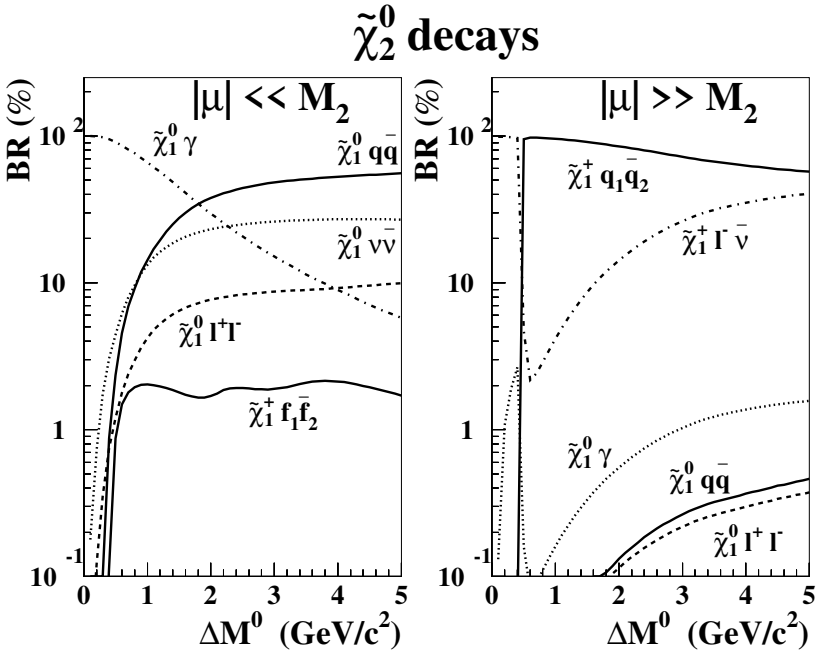

Figure 4: Predicted branching ratios of the decay modes of the second neutralino, with $M_{\tilde{\chi}_2^0} \simeq 50$ GeV/c^2, as a function of the mass difference between the $\tilde{\chi}_2^0$ and the $\tilde{\chi}_1^0$. The left and right plot refer to the higgsino-like and gaugino-like scenario respectively.

LEP centre-of-mass energy. The trigger efficiency for high momentum charged particles crossing the full depth of the TPC and the RICH is practically unity.

Lower limits on the mass of the chargino have been already published [11] under the hypothesis that it decays predominantly outside the DELPHI detector (in case of an heavy $\tilde{\nu}$ this corresponds to $\Delta M^{\pm} \lesssim 100$ MeV/c^2). For shorter lifetimes, the detection efficiency can be obtained by convoluting the efficiency for stable particles with the probability that the chargino passes through the barrel RICH before decaying.

4.2 Decay vertices inside the detector (kinks)

If the heavy charged particle decays inside the central tracking devices of DELPHI (at a radius between 10 cm and 1 m) then both the incoming and the outgoing track can be reconstructed, and the angle between the tracks can be calculated. This method was used in a DELPHI search for scalar tau leptons decaying into a light gravitino and an ordinary tau lepton [12]. For small $\Delta M^{\pm}$, however, the visible momentum of the decay products is quite small (typically less than 1 GeV/c), and the identification of the secondary track and, therefore, of the kink becomes more difficult. The selection criteria adopted in [12] have therefore been modified for the present search, exploiting the typical topology of these events: two particles emitted in opposite hemispheres decaying into one low-energy charged particle each.

A set of rather loose general requirements was imposed on the events in order to suppress the low energy background (beam-gas, beam-wall, etc), two-photon, e^+e^- and hadronic events:

- there must be at least one charged particle and not more than five;
- the visible energy must be above 10 GeV;

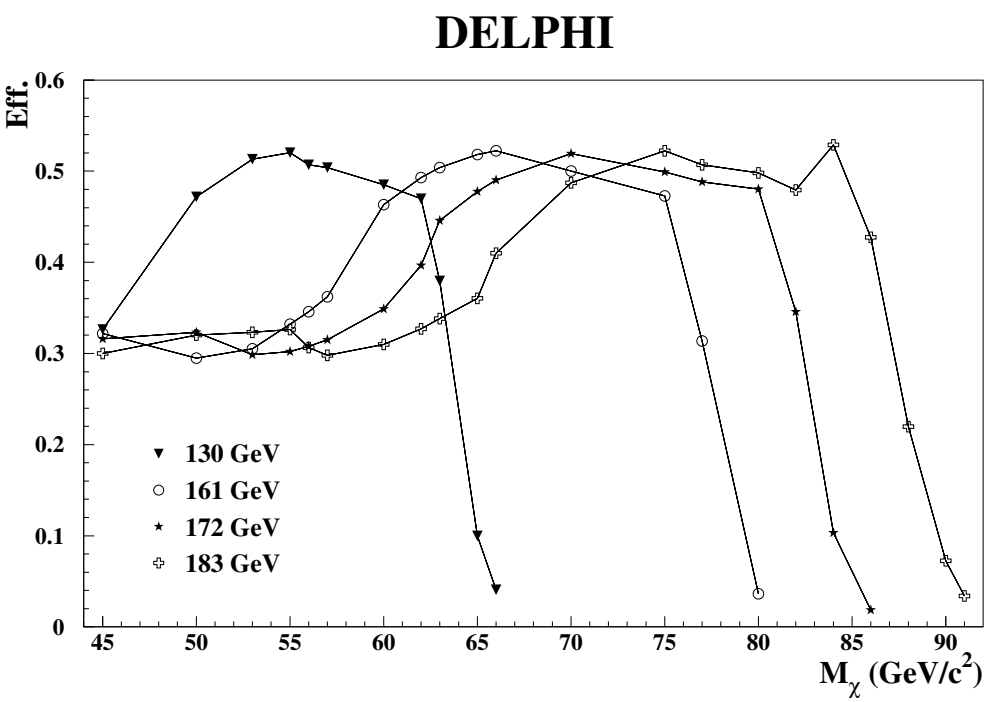

Figure 5: Efficiency for detecting a single heavy stable chargino in DELPHI (produced in pair in the e^+e^- rest frame), as a function of its mass and for the different centre-of-mass energies used in the analysis.

- the total energy in electromagnetic showers was required to be below 60 GeV;
- the transverse momentum with respect to the beam axis had to be greater than 5 GeV/c;
- the energy measured in the STIC must not exceed 10 GeV.

To compute the above quantities the reconstructed charged particles were required to have momenta above 100 MeV/c and impact parameters below 4 cm in the transverse plane and below 10 cm in the longitudinal direction (however, no requirement on the impact parameters were imposed to the reconstructed tracks in the following steps). Clusters in the calorimeters were interpreted as neutral particles if they were not associated to charged particles and if their energy exceeded 100 MeV.

All the charged particle tracks were grouped in clusters according to their measured point closest to the interaction vertex (starting point). The clustering procedure is described in [12]. Each cluster contains all tracks whose starting points differ by less than 2 cm. The starting point of a cluster is defined as the average of the starting points of its tracks. This procedure allows for clusters with a single track.

A cluster with only one track was considered a $\tilde{\chi}_1^+$ candidate if:

- the distance of the starting point from the beam spot, in the plane transverse to the beam axis (xy plane), $R_{\rm sp}^{\tilde{\chi}_1^+}$, was smaller than 10 cm;
- its momentum was greater than 20 GeV/c;
- the polar angle of the momentum had to satisfy $|\cos\theta| < 0.8$;
- the impact parameters of the track along the beam axis and in the plane perpendicular to it were less than 10 and 4 cm, respectively.

For each single track cluster fulfilling the above conditions, a search was made for a second cluster with starting point in the transverse plane beyond $R_{\rm sp}^{\tilde{\chi}_1^+}$, and an angular

separation between the directions defined by the beam spot and the starting points of the clusters smaller than 90° in the xy plane. This secondary cluster was assumed to be formed by the decay products of the $\tilde{\chi}_1^+$. Therefore, the $\tilde{\chi}_1^+$ candidate and the secondary cluster had to define a vertex. If the secondary cluster included more than one track, only the track with the highest momentum was used to search for the decay vertex or kink (crossing point with the $\tilde{\chi}_1^+$ track).

The crossing point was defined as the midpoint of the line segment connecting the points of closest approach in the xy plane between the two (possibly extrapolated) tracks: the candidate $\tilde{\chi}_1^+$ track and the selected track from the secondary cluster. The following conditions were required to define a good crossing point:

- the minimum distance between the tracks had to be smaller than 1 mm in the xy plane,
- the crossing point, the end point of the $\tilde{\chi}_1^+$ track and the starting point of its decay products were required to satisfy the following conditions:

$$\begin{array}{rcrcr} -10\,\mathrm{cm} & < & (R_{\mathrm{cross}} - R_{\mathrm{end}}^{\tilde{\chi}_1^+}) & < & 25\,\mathrm{cm} \\ -25\,\mathrm{cm} & < & (R_{\mathrm{cross}} - R_{\mathrm{sp}}^{\mathrm{dec.\,prod.}}) & < & 10\,\mathrm{cm} \end{array}$$

  where $R_{\mathrm{end}}^{\tilde{\chi}_1^+}$, R_{cross} and $R_{\mathrm{sp}}^{\mathrm{dec.\,prod.}}$ are the distance from the beam spot to the end point of the $\tilde{\chi}_1^+$ track, the crossing point of the tracks and the starting point of the tracks supposed to come from the decay products of the chargino, in the xy plane.

Reconstructed secondary vertices could also be the result of particles interacting in the detector material, or bremsstrahlung, giving a particle trajectory reconstructed in two separate track segments. To eliminate this kind of background, events with a good crossing point (kink) were subjected to additional requirements:

- to reject hadronic interactions, any secondary vertex reconstructed in the region of the detector where there is material must be outside a cone of half opening angle of 5°, with apex at the beam spot and centred around the kink direction;
- to reject photon radiation, in the case of secondary clusters with only one track, no neutral particle was allowed in a 1° cone around the direction of the missing momentum, defined by the difference between the momentum of the $\tilde{\chi}_1^+$ and that of the daughter;
- to reject segmented tracks, the angle between the tracks used to define a vertex, calculated at the crossing point, had to be larger than 2°.

Finally, for an event to be accepted, at least one charged particle must be found in each hemisphere (defined by the plane which contains the beam spot and is perpendicular to the line connecting the beam spot to the kink).

This selection was applied to samples of $\mathrm{e^+e^-} \to \tilde{\chi}_1^+\tilde{\chi}_1^-$ events, generated at $\sqrt{s} = 161$, 172 and 183 GeV and passed through the full DELPHI simulation and reconstruction chain. The efficiencies for the single vertex reconstruction as a function of the radial distance from the decay to the beam spot are plotted in figure 6a, where the case of a 65 GeV/c^2 chargino with $\Delta M^{\pm} \simeq 150$ MeV/c^2 has been taken as example. The selection efficiency ($\varepsilon^{\mathrm{sel}}$) is almost independent of the decay radius for radii between 30 and 90 cm for almost all the masses generated; it tends to decrease only when the mass of the chargino approaches the kinematical limit, because the momenta of the secondaries are not sufficiently enhanced by the reduced boost. The dependence of the selection efficiency on $\Delta M^{\pm}$ is weak for the values of $\Delta M^{\pm}$ within the range searched for with this

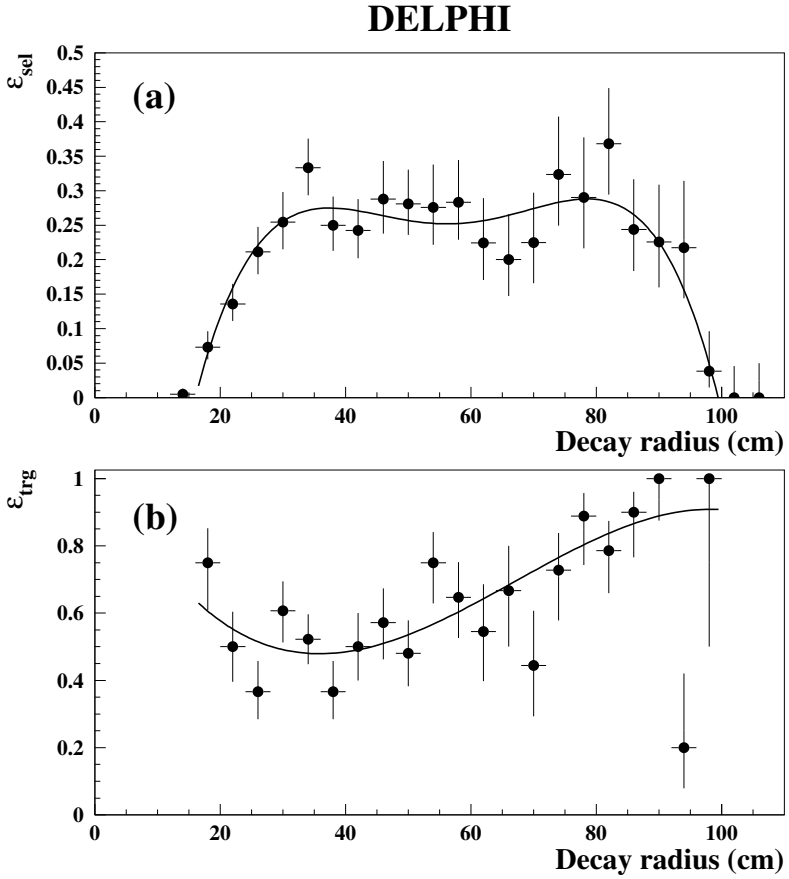

Figure 6: Efficiency for the kink reconstruction of a 65 GeV/c^2 chargino with $\Delta M^{\pm} \simeq 150$ MeV/c^2, as a function of the chargino decay radius, at the centre-of-mass energy of 183 GeV: (a) selection efficiency for the single arm; (b) single particle trigger efficiency for the selected kinks. The lines superimposed represent the result of the fit described in the text.

method. There is however some increase of the efficiency with increased $\Delta M^{\pm}$, as the mean momentum of the decay products gets higher.

The trigger efficiency ($\varepsilon^{\rm trg}$) depends on the mass of the chargino and on the centre-of-mass energy. It has been estimated with a simplified simulation of the single track trigger in DELPHI, taking the overall trigger efficiency as the logical OR of the trigger efficiencies of every single charged track in the event [21]. This is a conservative estimate because the possible contribution of all higher multiplicity triggers was neglected. The efficiency for triggering on the hemisphere of the kink, as a function of the decay radius of the chargino, is shown in figure 6b, for the same sample as in figure 6a. The radial dependence of both selection and trigger efficiencies was fitted with polynomials, allowing a different fit at every mass generated. The results of these fits were used in the analysis and the efficiencies for masses other than those simulated were obtained by interpolation.

4.3 Global efficiency for charginos with visible decay length

The selections in the search for long-lived charginos yield an efficiency $\varepsilon(x)$ which is a function of the decay radius x of the chargino. Each chargino produced in the e^+e^- collision can be selected by either one of the two searches: if it decays outside the RICH,

by the search for stable charged particles; if it decays inside the ID or the TPC, by the search for kinks. The global efficiency, which is a function of the decay radius, is given by the logical OR of the two selections.

To extrapolate the efficiency of the event selection to the points in the space of the SUSY parameters not fully simulated, a semi-analytic calculation was used. The distribution of the decay length of the chargino in the reference frame of DELPHI was derived analytically in the scenarios studied and for any given chargino mass, $\Delta M^{\pm}$ and centre-of-mass energy. These distributions were convoluted with the efficiencies of the experimental search methods $\varepsilon(x)$, as determined for the fully simulated events, giving the detection efficiency in any point of the space of the SUSY parameters.

As an example, figure 7 shows the combined detection and trigger efficiency at 183 GeV for $e^+e^- \to \tilde{\chi}_1^+\tilde{\chi}_1^-$, when the charginos are pure gauginos and $M_{\tilde{\nu}} = 1$ TeV/c^2, $M_{\tilde{\chi}} = 65$ or 80 GeV/c^2, as a function of $\Delta M^{\pm}$. The efficiencies displayed include both searches for long-lived charginos (for heavy stable particles and for kinks).

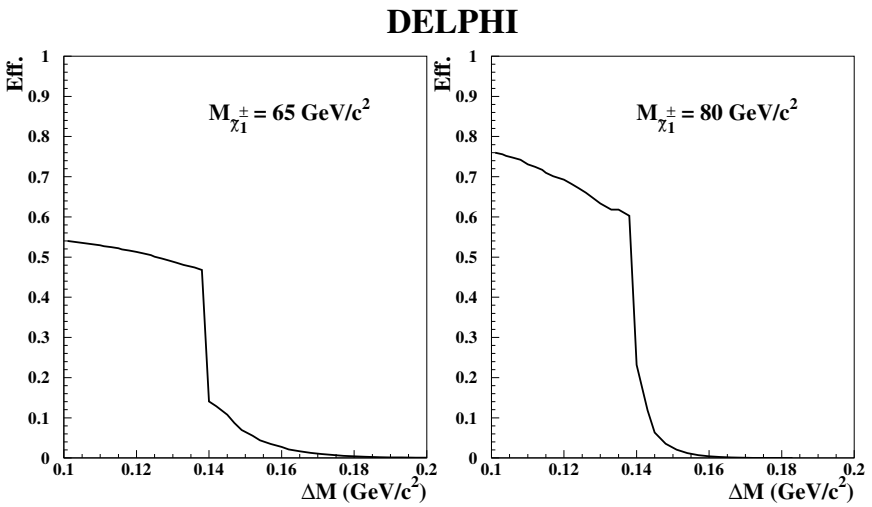

Figure 7: Total efficiency for detecting a long-lived charged gaugino in DELPHI using the analysis at 183 GeV as function of $\Delta M^{\pm}$ (that is of its lifetime) and in the approximation of heavy sneutrinos. The two masses of 65 and 80 GeV/c^2 have been chosen as examples.

4.4 Results

The search for heavy stable particles was performed with all the data collected at $\sqrt{s} = 130/136$, 161, 172 and 183 GeV. No candidates remained in the data, while 0.7 ± 0.3 background events were expected [11].

In the search for kinks, only data taken in 1996 and 1997 at the centre-of-mass energies of 161, 172 and 183 GeV were analysed. No events were selected, while the background expected at the three centre-of-mass energies was, respectively, 0.11 ± 0.11 , $0.04^{+0.11}_{-0.04}$ and 0.21 ± 0.14 events.

In the absence of candidates selected in any of the searches, the 95% confidence level (CL) upper limit is 3.0 events [22] for the whole statistics analysed. When this limit is considered together with the integrated luminosities, the expected cross-sections and efficiencies for different SUSY parameters, the 95% CL exclusion regions in the plane $(M_{\tilde{\chi}_1^+}, \Delta M^{\pm})$ shown in figure 12 can be derived. As far as the SUSY scenarios are con-

cerned, three cases were considered (see also section 3; here the results for gauginos are further subdivided according to the mass of the sneutrino):

1. low $|\mu|$, large $M_{1,2}$ and $M_{\tilde{\chi}_1^+} < M_{\tilde{\nu}}$, (higgsino-like);
2. high $|\mu|$, low M_2 and $M_{\tilde{\nu}} \geq 500$ GeV/c^2 (gaugino-like);
3. high $|\mu|$, low M_2 and $M_{\tilde{\chi}_1^+} < M_{\tilde{\nu}} < 500$ GeV/c^2 (gaugino-like).

In all cases, $\tan\beta$ was varied between 1 and 50, M_2 and $|\mu|$ between 0 and 100 TeV/c^2 and R_f between 1 and 10 (although for $R_f < 2$ it is not possible to have charged gauginos with masses close to that of the lightest neutralino). The lowest value of the cross-section obtained in the scan of the SUSY parameters for each scenario, at a given mass of the chargino, was used for the calculation, so that the limit obtained remains valid for all values of the parameters. The limits obtained in the third case are much less stringent than the other two, because a light sneutrino increases the chargino decay width through virtual $\tilde{\nu}$ exchange. Whenever $M_{\tilde{\nu}} < M_{\tilde{\chi}_1^+}$ the exchanged sneutrino becomes real and the lifetime drops: this region cannot be excluded by the search for long-lived charged particles.

Possible systematic biases of these limits have been considered. The relative statistical errors on the selection and trigger efficiencies propagate at the second order to the numerical value of the final limit [23]; this is expected to raise by no more than a fraction of a percent the upper limit of the cross-sections attainable and, for that reason, those errors were not taken into account further. The efficiencies found in the search for kinks can be slightly overestimated for $\Delta M^{\pm}$ smaller than those used in the full simulation, because in that case the mean momentum, and so the detectability, is lower. However, this would not affect the overall limits obtained, as this region is fully covered by the search for stable particles. Instead, at larger $\Delta M^{\pm}$ the efficiencies can be slightly underestimated; in that case the limits displayed in figure 12 are conservative (that is the confidence level is 95% or higher). The same holds for the trigger efficiency. In conclusion, the limits obtained are reliable, or conservative, in the whole space of the SUSY parameters spanned by the present search.

5 Search for charginos with ISR photons

To look for short-lived charginos close in mass to the lightest neutralino, events with a few low energy particles accompanied by an ISR photon at high transverse momentum were searched for. Samples of $e^+e^- \to \tilde{\chi}_1^+\tilde{\chi}_1^-$ events with initial (and final) state radiation were simulated with $\Delta M^{\pm}$= 0.3, 0.5, 1 and 3 GeV/c^2. The criteria used to search for such events in the data were then defined on the basis of these samples and the simulated background samples.

5.1 Charged and neutral particle selection

Tracks reconstructed in the detector were considered as charged particles, to be used in the subsequent analysis, if their momenta were above 100 MeV/c and known with an error below 100%, their impact parameters were below 4 cm in the transverse plane and below 10 cm in the longitudinal direction and if the tracks were at least 30 cm long.

To be accepted, neutral particles had to have an energy of at least 500 MeV. Both calorimetric showers and clear photon conversions in the material in front of the HPC were considered. Photon conversions were identified using the standard DELPHI algorithm [13]

which looks for a pair of tracks originating from a common secondary vertex and with an invariant mass compatible with zero.

Subdetector dependent criteria were used to reduce the rate of spurious neutral particles reconstructed from electronic noise in the calorimeters or, in the case of the HPC, from α-emission by radionuclides embedded in the lead of the converter material.

In the showers reconstructed by the HPC at least three of the nine layers must have given a signal; the first layer with a signal must be before the sixth HPC layer; not more than 90% of the total energy of the shower must be deposited in a single layer; the polar angle of the shower axis must point towards the main event vertex within 15°.

In the FEMC a signal was required in at least two towers. In the data collected since 1997 a more refined quality requirement was used, defining a frame of 3×3 glasses, centered on the barycentre of the shower: a shower was discarded if its energy was above 8 GeV and more than 94% of this energy was deposited in the central glass, or if it had no more than three glasses hit and these were all lined up in the same row or column.

In the STIC an energy of more than 2 GeV must be associated to the shower and at least two towers must be hit.

All neutral showers inside a cone with half opening angle of 5° were combined. The resulting shower was not considered an ISR photon candidate if the fraction of energy detected in the hadron calorimeter was above 10% of the total shower energy.

Given the reduced reconstruction and association efficiency of tracks in the two endcaps as compared to the barrel, spectator electrons from two-photon events can be seen as showers in the calorimeters without the corresponding track elements, thus faking neutral particles. Such electrons constitute a serious background to ISR photons, and care must be taken to reject these events.

5.2 Event selection

The analyses of the data collected before year 1997 and in 1997 have been done separately, with slightly different selection criteria. The tighter preselection cuts of 1997 were intended to reduce further the overall volume of the data used in the analysis, given the increased luminosity collected with respect to the previous years. The final selection of 1997 data also exploited the improved charged particle rejection in the forward regions which is obtained by trying to associate hits in the Silicon Tracker to the neutral showers.

5.2.1 Preselection

In the preselection, events were required to have at least two and at most ten charged particles. There should be an isolated photon candidate of at least 4 GeV, having a transverse energy above 2 GeV (above 4.5 GeV in the 1997 data at the centre-of-mass energy of 183 GeV) and a mass recoiling against it ($M_{\rm opp}$, defined by $M^2_{\rm opp} = E^2_{\rm cms} - 2E_{\rm cms}E_\gamma$) of at least 90 GeV/$c^2$. This photon had to be isolated from any other charged or neutral particle in the event by 15° or more. The visible energy of all particles excluding the photon must not exceed 8% of the available centre-of-mass energy. If all the particles in the event were in the same hemisphere inside a cone centered on the beam axis and with half opening angle of 60°, the event was discarded; this reduces the background coming from beam-gas or beam-wall interactions. To reject most of the two-photon background, also the fraction of the total visible energy within 30° of the beam axis (excluding the ISR photon candidate when inside that cone) was required to be less than 60%.

5.2.2 Selection

Following the preselection, in order to optimize signal efficiency and background rejection, more stringent selection criteria were imposed as follows.

- There must be at least two and at most six accepted charged particles and, in any case, not more than ten tracks in the event.
- To reject the bulk of the two-photon background, the transverse energy of the ISR photon was required to be greater than $(E_\gamma^T)^{\min}$, defined in eq. (1). Here $\theta_{\min}$ was taken as the minimum angle at which the photon shower is fully reconstructed in the STIC (1.82°).
- $M_{\rm opp}$ must be above 96 GeV/c^2. This was intended mainly to reduce the number of events with an on-shell Z recoiling against the photon.
- The photon was required to be isolated by at least 30° with respect to any other charged or neutral particle in the event.
- The sum of the energies of the particles emitted within 30° of the beam axis (E_{30}) was required to be less than 25% of the total visible energy. The photon was not considered in any of the two energy sums if its direction was inside that cone.
- If the ISR photon candidate was detected in the STIC, it must not be correlated with a signal in the Veto Counters.
- In the data collected during 1997, if the ISR photon candidate was at an angle between 10° and 25° from the beam, the region where the TPC cannot be used in the tracking, it must not be correlated with hits in the Silicon Tracker.
- The visible energy of the event, excluding the photon, must be below 5% of $E_{\rm cms}$. For $\Delta M^\pm < 1$ GeV/c^2 this fraction was reduced to 2%.

Figures 8, 9 and 10 show the distributions of some of the variables used for the selection in the preselected samples at 161, 172 and 183 GeV respectively. The data are compared with the SM expectation, normalized to the same luminosity. The agreement is good in almost all distributions. The simulated two-photon interactions giving hadrons via the QPM process with and without ISR were compared. It was evident that the small excess of real data in the first bins of the distributions of E_{30} and $(E_{\rm vis} - E_\gamma)$ can be, at least qualitatively, explained by the lack of ISR in some of the simulated two-photon samples. At present there are no generators available, however, which correctly describe the ISR in these processes.

The corresponding distributions for the signal with $M_{\tilde{\chi}_1^\pm} = 50$ GeV/c^2 and $\Delta M^\pm = 1$ GeV/c^2, taken as an example, are shown to the right in the same figures. The histograms of the visible energy are shown for the three mass differences of 0.3, 1 and 3 GeV/c^2, since the energy of the visible decay products depends on $\Delta M^\pm$.

For the background estimates at $\sqrt{s} = 130$ and 136 GeV, the problems with the simulated samples were more important: many of them were originally generated with insufficient statistics or with stricter requirements than those used in the subsequent analysis. No detailed comparison of the distributions of the data with respect to the simulation was meaningful at those energies.

5.3 Results

The results of the selection, when applied to data and simulated background at all the centre-of-mass energies, are shown in table 1. Six candidate events remain in the data after the selection for $1 \leq \Delta M^\pm \leq 3$ GeV/c^2 (one in the sample at 136 GeV collected in

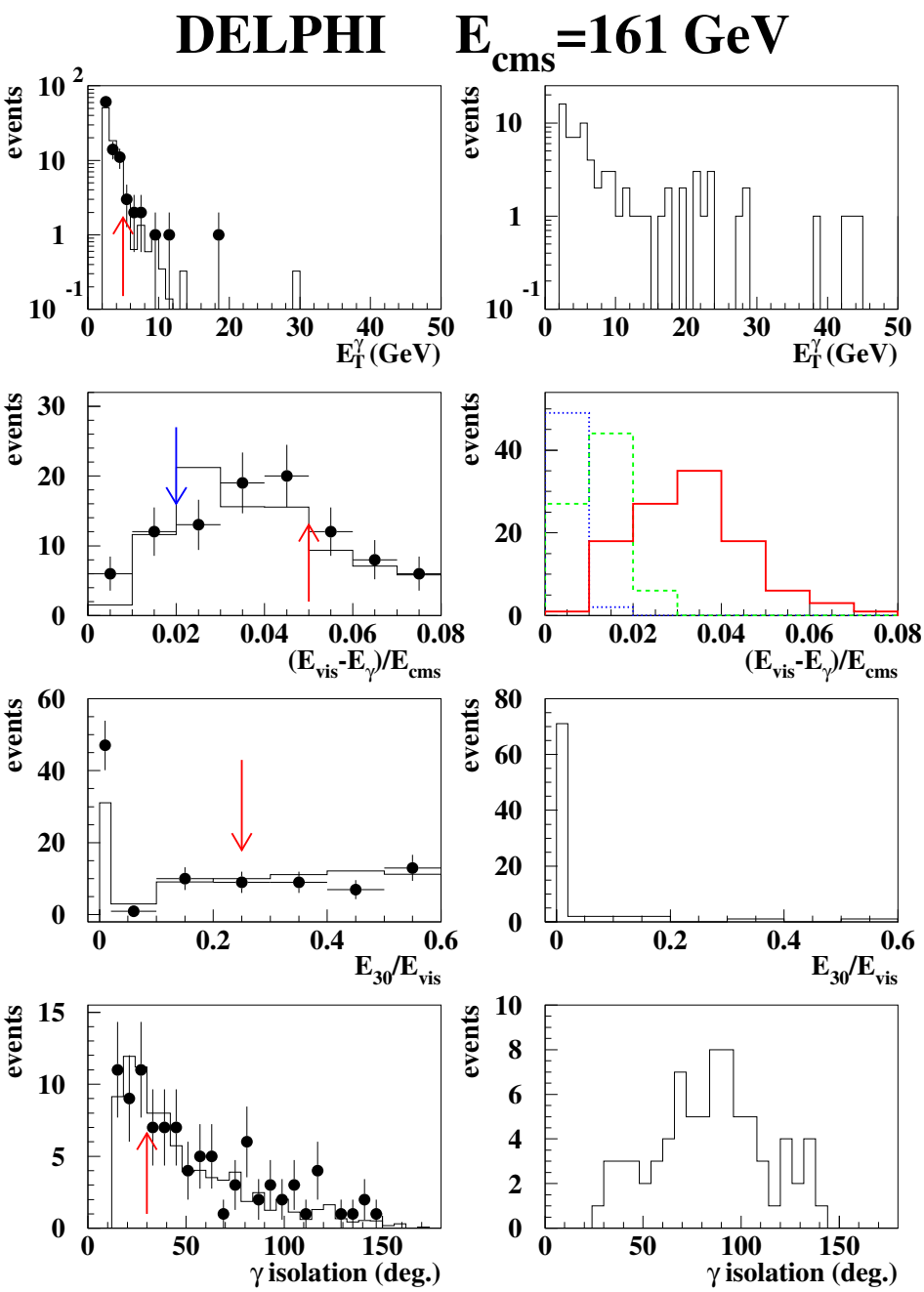

Figure 8: Some of the variables used in the selection at 161 GeV. In the left plots the data (dots) are compared with the SM expectations. On the right, as an example, the corresponding distributions (with arbitrary normalization) are shown for the signal with $M_{\tilde{\chi}_1^+} = 50$ GeV/c^2 and $\Delta M^{\pm} = 1$ GeV/c^2. In the plot of the visible energy (second row) all three mass splittings are shown: dotted, $\Delta M^{\pm} = 0.3$ GeV/c^2; dashed, $\Delta M^{\pm} = 1$ GeV/c^2; full line, $\Delta M^{\pm} = 3$ GeV/c^2.

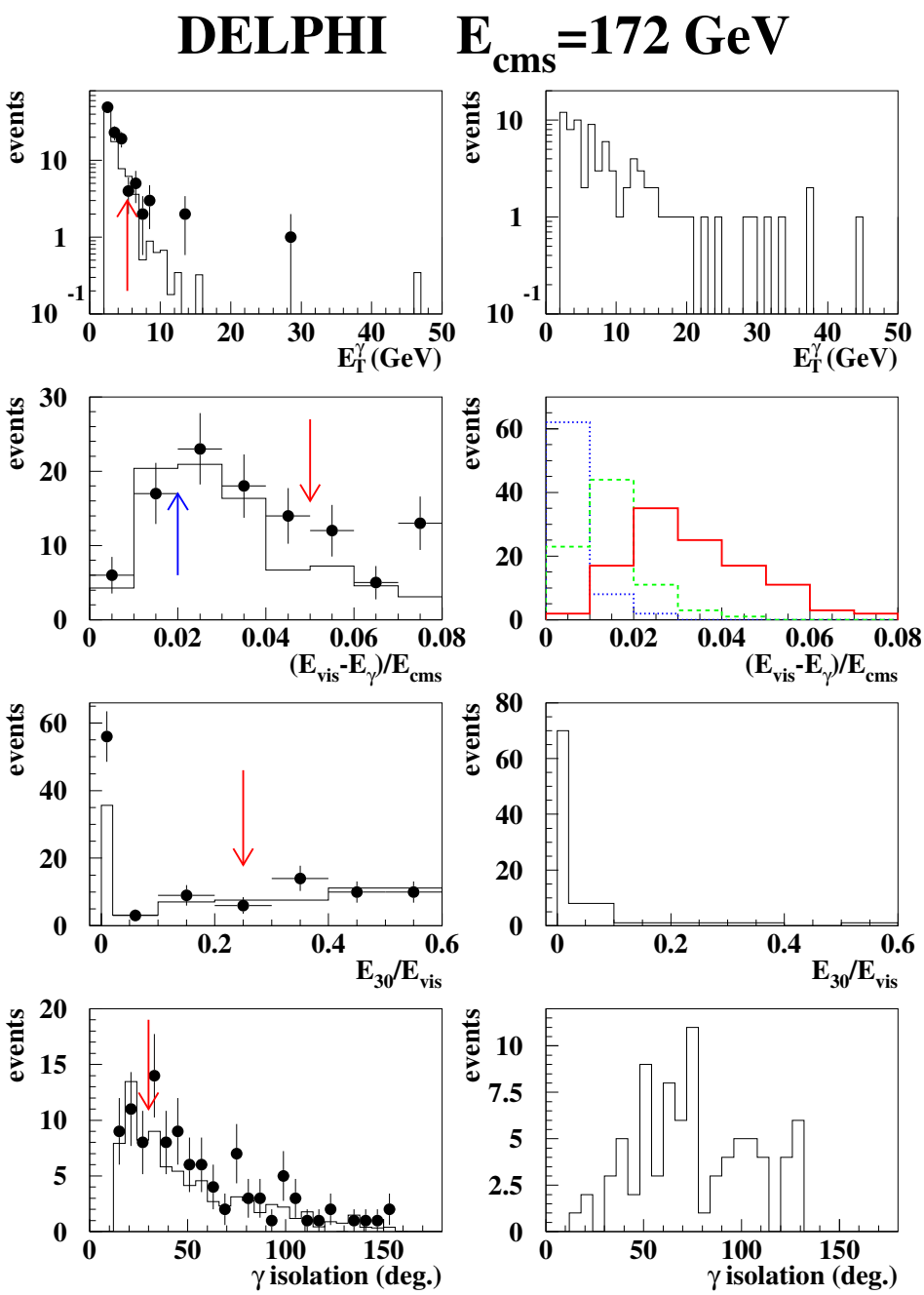

Figure 9: Same as figure 8, but data and simulation refer to the samples at 172 GeV.

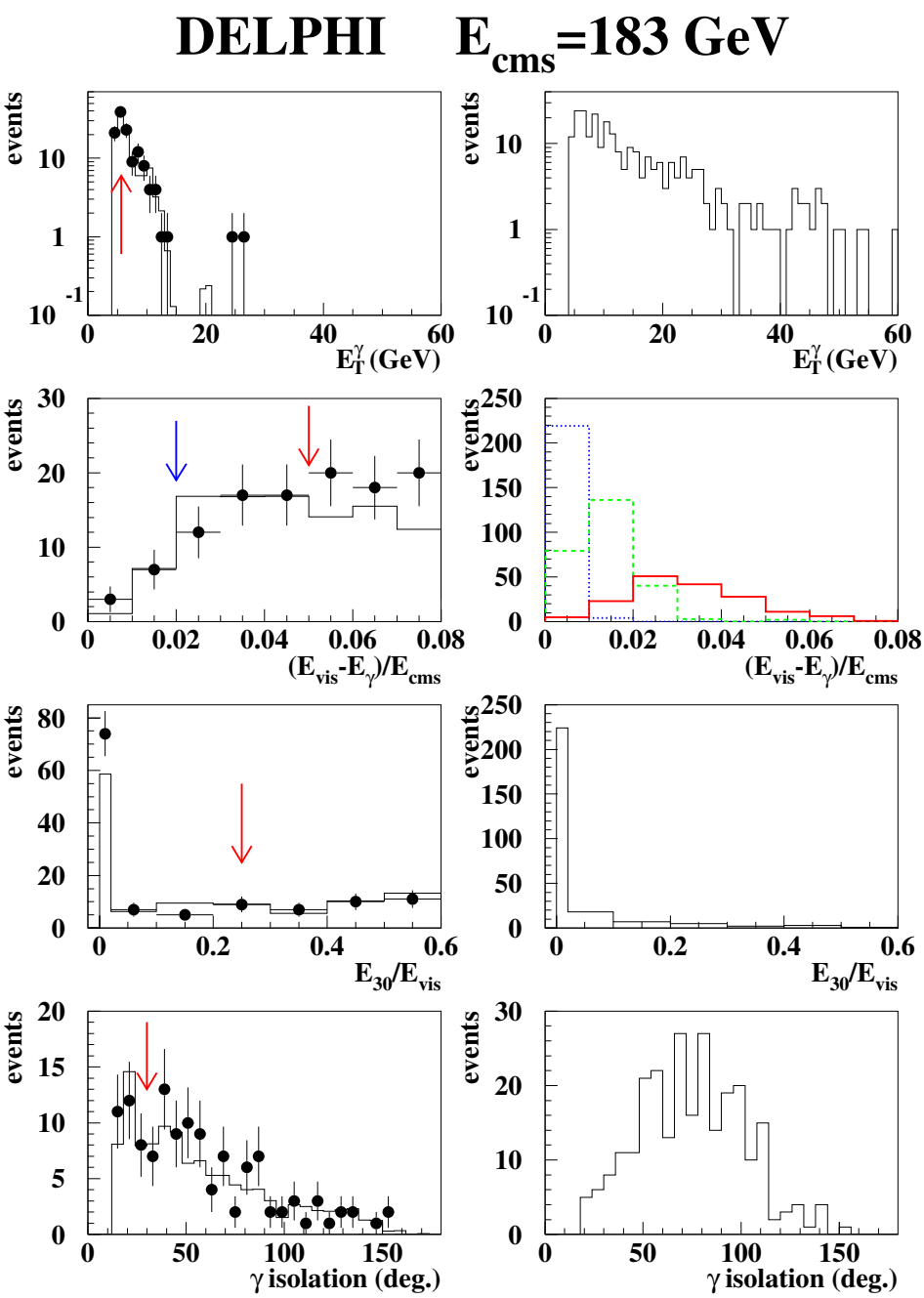

Figure 10: Same as figure 8, but data and simulation refer to the samples at 183 GeV. The cut on the transverse energy of the photon in the preselection is tighter than the one used in the previous plots at lower centre-of-mass energies.

1995, one at 172 GeV and four at 183 GeV). Some of their properties are summarized in table 2. Only two of them pass also the stricter requirements for smaller $\Delta M^{\pm}$ (both at 183 GeV). There is no significant excess above the SM expectations in either selection. The SM background remaining at the end of the selection is almost entirely composed of two-photon interactions.

$E_{\rm vis} - E_\gamma < 5\% \cdot E_{\rm cms}$ $(1 \leq \Delta M^{\pm} \leq 3$ GeV/$c^2)$		$E_{\rm vis} - E_\gamma < 2\% \cdot E_{\rm cms}$ $(\Delta M^{\pm} < 1$ GeV/$c^2)$	
Data	**Σ backgrounds**	**Data**	**Σ backgrounds**
$E_{\rm cms} = 130/136$ GeV $\quad (\int \mathcal{L} = 11.7$ pb$^{-1})$			
1	0.84 ± 0.84	0	$\simeq 0$
$E_{\rm cms} = 161$ GeV $\quad (\int \mathcal{L} = 9.7$ pb$^{-1})$			
0	1.12 ± 0.38	0	0.45 ± 0.21
$E_{\rm cms} = 172$ GeV $\quad (\int \mathcal{L} = 9.9$ pb$^{-1})$			
1	0.64 ± 0.18	0	0.11 ± 0.06
$E_{\rm cms} = 183$ GeV $\quad (\int \mathcal{L} = 50.0$ pb$^{-1})$			
4	2.96 ± 0.88	2	0.44 ± 0.21

Table 1: Results of the selection on the data and on the sum of the expected SM backgrounds. The integrated luminosity is the one used for the analysis.

At 130/136 GeV some of the background samples were either missing or had requirements at the generation level stricter than those used later in the analysis and the background quoted in the first line of table 1 is likely to be underestimated.

The selection efficiency ($\varepsilon^{\rm sel}$) for charged higgsinos and gauginos at $\sqrt{s} = 183$ GeV, determined by using the samples of simulated events is shown in figure 11 as a function of the mass of the chargino and of $\Delta M^{\pm}$. Similar efficiencies have been obtained at the other centre-of-mass energies. It must be stressed that the very low signal efficiency comes from the requirement of having an energetic ISR photon radiated at visible angles. As the mass of the chargino increases, the energy of the photon decreases, thus lowering the overall event selection efficiency. The selection efficiency for gauginos, in the case of a heavy sneutrino, is higher than for higgsinos, even though the decays are similar in the two scenarios, because the gaugino cross-section resonates more strongly around the Z pole, leading to more frequent ISR radiation. However, the gaugino efficiency is

$E_{\rm cms}$ (GeV)	$N_{\rm charged}$	$N_{\rm neutral}$	$E_{\rm vis}$ (GeV)	E_γ (GeV)	θ_γ (deg.)	$\mathrm{IP}_1^{r\phi}$ (cm)	$\mathrm{IP}_2^{r\phi}$ (cm)
136	2	2	40.1	34.1	165.5	-0.18 ± 0.03	0.62 ± 0.06
172	2	2	12.6	7.9	56.8	0.00 ± 0.01	0.00 ± 0.01
183	2	1	54.3	53.4	10.6	-0.05 ± 0.03	0.01 ± 0.02
183	2	1	11.7	8.4	52.2	-0.01 ± 0.03	-0.01 ± 0.01
183	2	2	13.2	7.0	124.9	0.05 ± 0.04	0.00 ± 0.01
183	2	1	13.2	5.8	85.5	0.00 ± 0.01	0.00 ± 0.01

Table 2: Some of the properties of the events remaining in the data after the selection: the centre-of-mass energy, the number of charged and neutral particles in the event, the energy and the polar angle of the photon, the impact parameters in the plane $r\phi$ of the two charged tracks.

significantly smaller than the one shown in the figure when the mass of the sneutrino is close to the mass of the chargino: light sneutrinos would enhance the fraction of leptonic decays, which have additional missing energy and then a lower efficiency for the same $\Delta M^{\pm}$. All this was taken into account when computing the exclusion limits.

Below transverse momenta of 1-2 GeV/c the single track trigger efficiency of DELPHI starts to decrease [21]. The events searched for have few tracks of low energy (besides the energetic photon); for that reason, a dedicated and detailed study of the trigger performances at low visible transverse energy was carried out. The trigger efficiencies for events with a visible transverse energy similar to the one of the system accompanying the ISR photon in the signal samples which pass the selection cuts, were computed from all the data collected at LEP2. This study had to be repeated for every new year of data taking, since the definitions of the decision functions and the downscaling factors applied in case of noise during the data acquisition can affect the results. The sample of events with independent trigger signals from any of the calorimeters was used to compute the efficiency for the tracking components of the trigger. The overall trigger efficiency for the signal ($\varepsilon^{\rm trg}$) was then estimated as the logical OR of the single photon trigger efficiency [24] and the trigger efficiency for events in which there are only low energy tracks. For the signal events considered here, the estimated overall trigger efficiency varies between 82% and 98%.

5.4 Exclusion limits in the search with the ISR tag

Since there was no evidence for a signal at any of the centre-of-mass energies studied, limits were derived on the pair production of charginos nearly mass-degenerate with the LSP.

5.4.1 Method

Although the cross-section is relatively high for all chargino masses (see figure 1), it is important to combine the data taken at all energies, because of the low signal efficiency. The method used to obtain a combined limit from the data taken at the different centre-of-mass energies is the following.

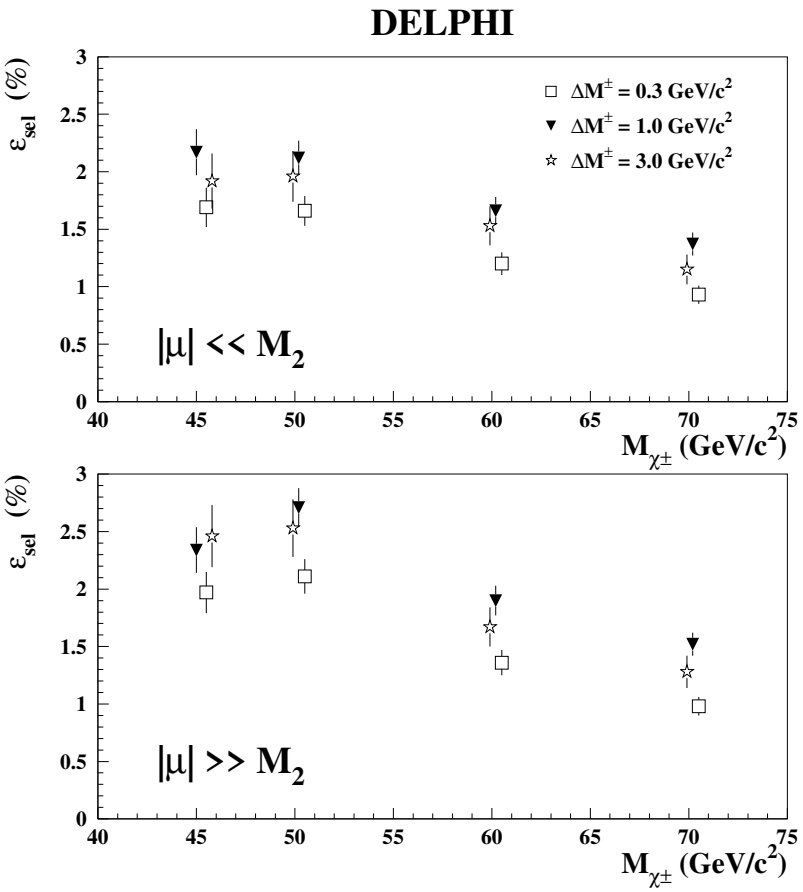

Figure 11: Selection efficiencies for charged higgsinos and gauginos at 183 GeV as a function of their mass and mass difference with the lightest neutralino. This gaugino efficiency is valid only in the approximation of heavy sneutrinos; for light sneutrinos a different value is used.

The number of candidates observed at each centre-of-mass energy is distributed according to a Poissonian. The (Bayesian) probability density of the true mean value for the number of signal events in the data ($N_{\rm sig}$) is derived according to [25], given the number of observed events and the expected number of background events at each $E_{\rm cms}$. The error on the expected background content was taken into account by assigning a Bayesian probability density to different values of the background and weighting the $N_{\rm sig}$ densities by the background density. The background densities used were taken to be Gaussian at every $E_{\rm cms}$, with standard deviations equal to the errors reported in table 1.

The total number of expected signal events is

$$N_{\rm exp} = \sum \sigma_i \mathcal{L}_i \, \varepsilon^{\rm sel} \varepsilon^{\rm trg} \tag{4}$$

where i runs over all the centre-of-mass energies. The statistical errors on the selection efficiencies completely dominate over the errors on the integrated luminosities and trigger efficiencies, which were neglected. For the cross-sections, the lowest values obtained in the scan of the SUSY parameters were used. $N_{\rm exp}$ was then assigned a Bayesian probability density, based on the binomial statistics relevant in the calculation of $\varepsilon^{\rm sel}$, and assuming equal a priori probabilities.

The two probability densities for $N_{\rm sig}$ and $N_{\rm exp}$ are independently determined, and the probability that $N_{\rm sig} < N_{\rm exp}$ can therefore be obtained by convoluting these two densities

using Monte-Carlo techniques. If this probability, in a given scenario, is equal to η for a point in the plane $(M_{\tilde{\chi}_1^+}, \Delta M^{\pm})$, then the point is excluded at the confidence level η.

In this way, confidence levels of exclusion were derived for the mass points where a full simulation of the signal had been performed. Between these points an interpolation, based on SUSYGEN events without full detector simulation, was used to obtain the limit.

5.4.2 Limits

Table 3 gives the 95% CL lower limits on the mass of the chargino for each of the three scenarios considered and for the different $\Delta M^{\pm}$ ranges. To compute the efficiencies, event samples have been generated at fixed values of the mass of the chargino and of $\Delta M^{\pm}$. While it is straightforward to interpolate between simulated points at the same $\Delta M^{\pm}$ and different $M_{\tilde{\chi}_1^+}$, it is more difficult in the case of different $\Delta M^{\pm}$ because of the different Q-values in the chargino decay. For this reason, a limit was calculated for each $\Delta M^{\pm}$ simulated by interpolation in $M_{\tilde{\chi}_1^+}$, but no interpolation in $\Delta M^{\pm}$ was done. Instead, the limit between any two simulated $\Delta M^{\pm}$ was conservatively taken as the the lower of the corresponding two $M_{\tilde{\chi}_1^+}$ limits, giving a step-like exclusion contour. In particular, no limit was derived below the minimum $\Delta M^{\pm}$ used in the simulation; however, using a small sample of simulated events it has been verified that those efficiencies drop quickly below that lowest $\Delta M^{\pm}$, at the centre-of-mass energies studied in this paper.

	$\lvert\mu\rvert \ll M_2$	$\lvert\mu\rvert \gg M_2$ $M_{\tilde{\nu}} > 500$ GeV/c^2	$\lvert\mu\rvert \gg M_2$ Any $M_{\tilde{\nu}} > M_{\tilde{\chi}_1^+}$
$0.3 \leq \Delta M^{\pm} < 0.5$ GeV/c^2	48.0 GeV/c^2	62.6 GeV/c^2	-
$0.5 \leq \Delta M^{\pm} < 1.0$ GeV/c^2	48.0 GeV/c^2	62.6 GeV/c^2	49.4 GeV/c^2
$1.0 \leq \Delta M^{\pm} \leq 3.0$ GeV/c^2	49.9 GeV/c^2	60.6 GeV/c^2	48.2 GeV/c^2

Table 3: 95% CL lower limits on the mass of the chargino obtained with the search for soft particles accompanied by an energetic ISR photon, in the three scenarios in which a mass-degeneracy with the neutralino is possible.

When the chargino is a gaugino and the mass of the sneutrino is above but close to $M_{\tilde{\chi}_1^+}$, the decay $\tilde{\chi}_1^+ \to \tilde{\chi}_1^0 l^+ \nu_l$, mediated by a virtual $\tilde{\nu}$, is enhanced with respect to the branching ratios shown in figure 3. In that case there are two invisible particles which carry away the energy and the visible lepton is usually softer than the pion of the two-body decay $\tilde{\chi}_1^+ \to \tilde{\chi}_1^0 \pi^+$. For this reason the selection efficiency becomes lower with a light sneutrino with mass above the chargino mass and the limit has been set only down to $\Delta M^{\pm} = 500$ MeV/c^2 in table 3.

If the sneutrino is lighter than the chargino, whether or not it is the LSP, the dominant decay mode is the two-body $\tilde{\chi}_1^+ \to l^+ \tilde{\nu}$, where the sneutrino and its decay products are all invisible. Although not computed explicitely here, the detection efficiencies in the scenario $M_{\tilde{\nu}} < M_{\tilde{\chi}}$ are expected to be similar to the ones derived in the high $M_{\tilde{\nu}}$ approximation at the lowest $\Delta M^{\pm}$ studied in this paper (where the two-body decay $\tilde{\chi}_1^+ \to \tilde{\chi}_1^0 \pi^+$ dominates). They are expected instead to be slightly lower at the largest $\Delta M^{\pm}$ studied in this paper

(where the upper limit on the visible energy has more effect on two-body decays than on three-body ones).

All these results take into account a variation of $\tan\beta$ between 1 and 50 and a variation of the M_1, M_2 and μ parameters so that the mass difference between the chargino and the neutralino remains below 3 GeV/c^2 and $M_2 \leq 2M_1 \leq 10M_2$.

As anticipated in section 2, the limitations of some of the two-photon generators used lead to an underestimate of the SM background in the region of high p_T ISR where the signal is expected. There is no evidence of any signal, however, and when deriving exclusion limits the only bias expected because of the somewhat inadequate simulation is that the mass limits are likely to be underestimated. In other words, the limits are conservative, in the sense that with a more precise background simulation their confidence level would be likely to exceed 95%. No attempt to compensate for this effect has been made.

Figure 12 shows these limits together with the ones obtained in the search for long-lived charginos. For completeness, also shown are the limits obtained at LEP1 [5,6] and the results of the search for high $\Delta M^{\pm}$ charginos in DELPHI [4].

6 Conclusions

Charginos nearly mass-degenerate with the lightest neutralino (assumed to be the LSP) have been searched for using the data collected by the DELPHI experiment during the runs of LEP above the Z pole energy from 1995 to 1997. Two different approaches were used.

For extremely small mass differences ($\Delta M^{\pm} \leq 200$ MeV/c^2) the information contained in the long lifetime of the chargino (decay length) was exploited. The search for heavy particles decaying outside the central subdetectors of DELPHI used the specific ionization of the tracks in the TPC and the light cone produced in the RICH detector. Chargino decays, between about 15 cm and 1 m, would be seen as kinks in the tracks reconstructed in the central tracking detectors of DELPHI. No candidate events were found in the data collected at 130, 136, 161, 172 and 183 GeV using the first analysis, or at 161, 172 and 183 GeV using the second analysis.

When the lifetime is so short that the decay vertex cannot be seen inside the sensitive devices of DELPHI and $\Delta M^{\pm}$ is too small ($0.3 < \Delta M^{\pm} < 3$ GeV/c^2) to be selected by the usual criteria adopted in the search for charginos, some events can still be recovered by looking for the typical topologies of the chargino decays at low $\Delta M^{\pm}$ accompanied by a high energy photon radiated from the initial state. The ISR signature reduces the otherwise overwhelming two-photon background to acceptable rates, although it also strongly affects the signal efficiency. It is necessary to combine all the statistics collected so far at the different LEP2 centre-of-mass energies to achieve sufficient sensitivity. No evidence of a signal has been found in the data collected by DELPHI at the centre-of-mass energies of 130, 136, 161, 172 and 183 GeV.

The regions of the plane $M_{\tilde{\chi}_1^+}$ vs. $\Delta M^{\pm}$ excluded at the 95% CL by the combination of these searches in DELPHI are summarized in figure 12. There is still an inaccesible region at, approximately, 200 MeV/$c^2 < \Delta M^{\pm} < 300$ MeV/c^2. With the higher statistics available and the increased boost of the decay products of the chargino, provided by the raised centre-of-mass energy, this region is likely to be explored with the use of data from 1998 onwards.

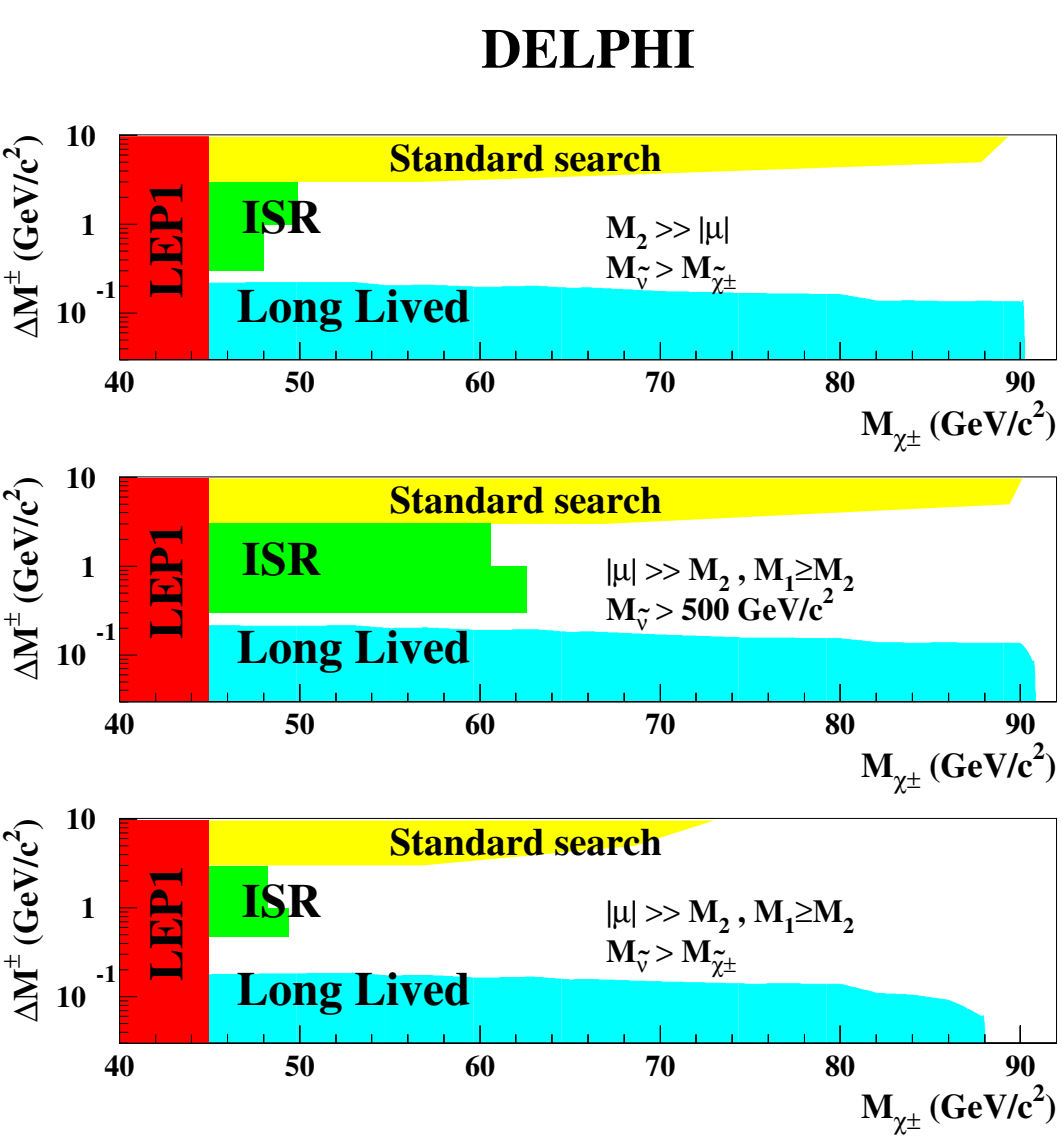

Figure 12: Regions in the plane ($M_{\tilde{\chi}_1^+}$,$\Delta M^{\pm}$) excluded by DELPHI at the 95% CL using: the search for high $\Delta M^{\pm}$ charginos; the search for soft particles accompanied by ISR; the search for long-lived charginos. The three scenarios are the ones which allow low $\Delta M^{\pm}$: the lightest chargino is a higgsino; the lightest chargino is a gaugino and $M_{\tilde{\nu}} > 500$ GeV/c^2; the lightest chargino is a gaugino and $M_{\tilde{\nu}} \geq M_{\tilde{\chi}_1^+}$.

Acknowledgements

We are greatly indebted to our technical collaborators, to the members of the CERN-SL Division for the excellent performance of the LEP collider, and to the funding agencies for their support in building and operating the DELPHI detector.
We acknowledge in particular the support of
Austrian Federal Ministry of Science and Traffics, GZ 616.364/2-III/2a/98,
FNRS–FWO, Belgium,
FINEP, CNPq, CAPES, FUJB and FAPERJ, Brazil,
Czech Ministry of Industry and Trade, GA CR 202/96/0450 and GA AVCR A1010521,
Danish Natural Research Council,
Commission of the European Communities (DG XII),
Direction des Sciences de la Matière, CEA, France,
Bundesministerium für Bildung, Wissenschaft, Forschung und Technologie, Germany,
General Secretariat for Research and Technology, Greece,
National Science Foundation (NWO) and Foundation for Research on Matter (FOM), The Netherlands,
Norwegian Research Council,
State Committee for Scientific Research, Poland, 2P03B06015, 2P03B03311 and SPUB/P03/178/98,
JNICT–Junta Nacional de Investigação Científica e Tecnológica, Portugal,
Vedecka grantova agentura MS SR, Slovakia, Nr. 95/5195/134,
Ministry of Science and Technology of the Republic of Slovenia,
CICYT, Spain, AEN96–1661 and AEN96-1681,
The Swedish Natural Science Research Council,
Particle Physics and Astronomy Research Council, UK,
Department of Energy, USA, DE–FG02–94ER40817.

References

[1] H. P. Nilles, Phys. Rep. **110** (1984) 1;
H.E. Haber and G.L. Kane , Phys. Rep. **117** (1985) 75.

[2] P.F. Smith, *et al.*, Nucl. Phys. **B206** (1982) 333.

[3] DELPHI Coll., P. Abreu *et al.*, Phys. Lett. **B382** (1996) 323;
DELPHI Coll., P. Abreu *et al.*, Phys. Lett. **B387** (1996) 651.

[4] DELPHI Coll., P. Abreu *et al.*, Eur. Phys. J. **C1** (1998) 1;
DELPHI Coll., P. Abreu *et al.*, Phys. Lett. **B446** (1999) 75.

[5] Particle Data Group, C. Caso et al., Eur. Phys. J. **C3** (1998) 1.

[6] J.F. Grivaz, in "Perspectives on Supersymmetry", World Scientific Publishing Co., G.L. Kane ed. (1998) 179;
M. Drees and X. Tata, Phys. Rev. **D43** (1991) 2971.

[7] A. Brignole, L.E. Ibañez and C. Muñoz, Nucl. Phys. **B422** (1994) 125, erratum *ibid.* **B436** (1995) 747.

[8] C.H. Chen, M. Drees and J.F. Gunion, Phys. Rev. **D55** (1997) 330, erratum, UCD-99-2 and hep-ph/9902309.
bibitemgiudice G.F. Giudice, M.A. Luty, H. Murayama, R. Rattazzi, CERN-TH/98-337 (1998).

[9] C.H. Chen, M. Drees and J.F. Gunion, Phys. Rev. Lett. **76** (1996) 2002.

[10] K. Riles *et al.*, Phys. Rev. **D42** (1990) 1.

[11] DELPHI Coll., P. Abreu *et al.*, Phys. Lett. **B444** (1998) 491.

[12] DELPHI Coll., P. Abreu *et al.*, Eur. Phys. J. **C6** (1999) 385;
DELPHI Coll., P. Abreu *et al.*, CERN-EP/98-170 (1998), accepted by Eur. Phys. J. **C**.

[13] DELPHI Coll., P. Aarnio, *et al.*, Nucl. Inst. Meth. **A303** (1991) 233;
DELPHI Coll., P. Abreu *et al.*, Nucl. Inst. Meth. **A378** (1996) 57, erratum *ibid.* **A391** (1997) 281.

[14] A.C. Benvenuti *et al.*, IEEE Trans. Nucl. Sci. **40** (1993) 537.

[15] T. Sjöstrand, Comp. Phys. Comm. **82** (1994) 74;
T. Sjöstrand, "PYTHIA 5.7 and JETSET 7.4: Physics and Manual", CERN TH 7112-93 (1995), LU-TP-95-20.

[16] "DELSIM users guide and reference manual", DELPHI 89-15 PROG 130 and 89-69 PROG 143.

[17] S. Katsanevas and S. Melachroinos in "Physics at LEP2", CERN/96-01 (Vol.2) 328;
S. Katsanevas and P. Morawitz, Comp. Phys. Comm. **122** (1998) 227.

[18] S. Thomas and J.D. Wells, Phys. Rev. Lett. **81** (1998) 34.

[19] F.A. Berends, P.H. Daverveldt and R. Kleiss, Nucl. Phys. **B253** (1985) 421;
Comp. Phys. Comm. **40** (1986) 271, 285 and 309.

[20] S. Nova, A. Olshevski and T. Todorov, "Monte-Carlo Event Generator for Two Photon Physics", DELPHI 90-35 PROG 152.

[21] V. Bocci *et al.*, Nucl. Inst. Meth. **A362** (1995) 361.

[22] Particle Data Group J.J. Hernandez et al., Phys. Rev. **D54** (1996) 1;
O. Helene, Nucl. Instr. Meth. **212**, 319 (1983).

[23] R.D. Cousins and V.L. Highland, Nucl. Inst. Meth. **A320** (1992) 331.

[24] DELPHI Coll., P. Abreu *et al.*, Zeit. Phys. **C74** (1997) 577;
DELPHI Coll., W. Adam *et al.*, Phys. Lett. **B380** (1996) 471;
P. Ferrari *et al.*, "Analysis of the single photon channel at LEP2", DELPHI 98-76 CONF 144.

[25] V.F. Obraztsov, Nucl. Inst. Meth. **A316** (1992) 388, erratum *ibid.* **A399** (1997) 500.